U.S. Department of Transportation

Federal Railroad Administration

Office of Research, Development and Technology
Washington, DC 20590

# Abdomen Impact Testing of the THOR-50M Anthropomorphic Test Device

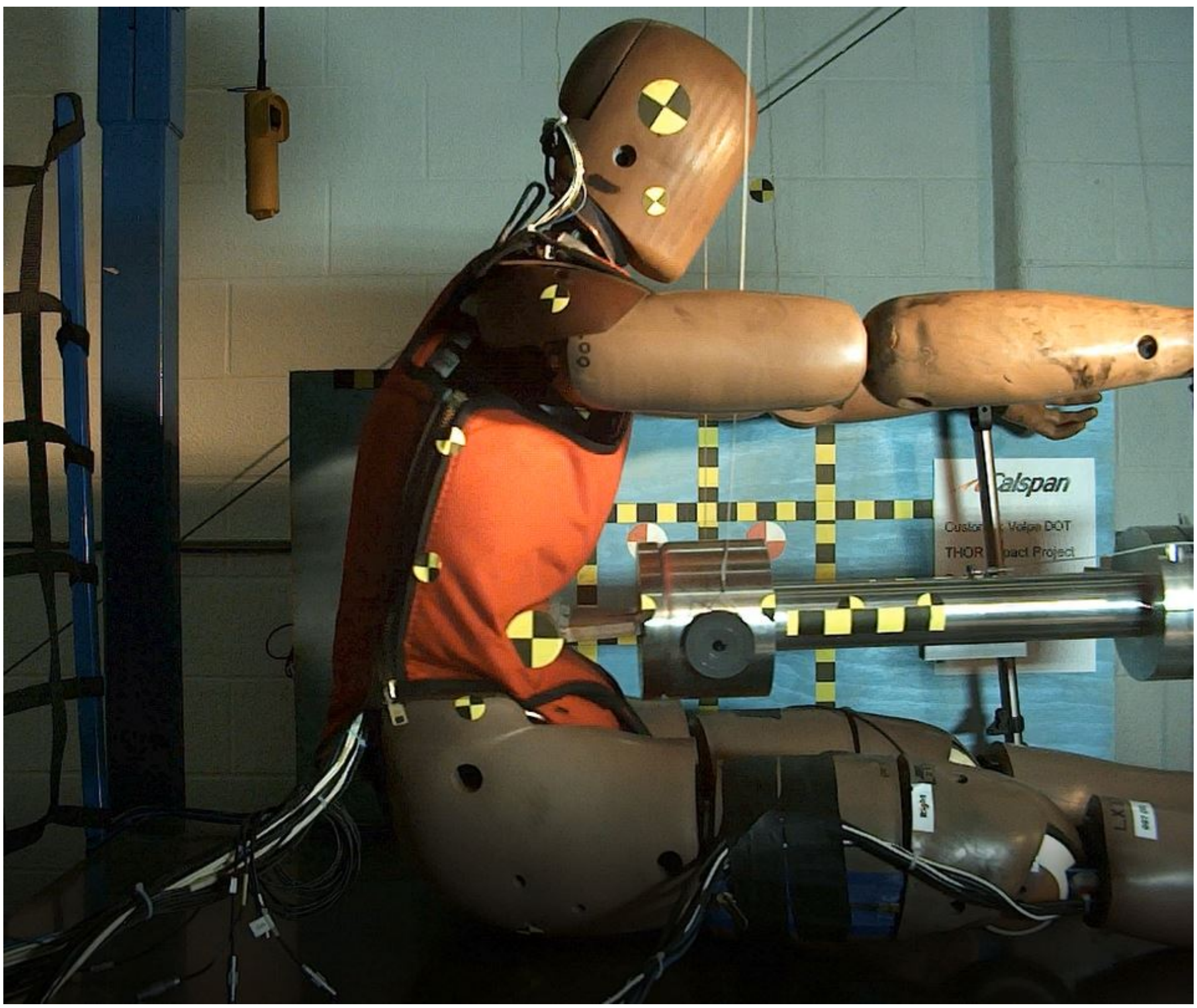

DOT/FRA/ORD-21/08

Final Report | February 2021

NOTICE



NOTICE

| REPORT DOCUMENTATION PAGE | | | Form Approved<br>OMB No. 0704-0188 |
|---|---|---|---|



| **1. REPORT DATE** *(DD-MM-YYYY)* | **2. REPORT TYPE** | **3. DATES COVERED** *(From - To)* |
|---|---|---|
| | Technical Report | 02/27/20 to 05/19/20 |

| **4. TITLE AND SUBTITLE** | |
|---|---|
| Abdomen Impact Testing of the THOR-50M Anthropomorphic Test Device | **5a. CONTRACT NUMBER**<br>6913G620P800065 |
| | **5b. GRANT NUMBER** |
| | **5c. PROGRAM ELEMENT NUMBER** |
| **6. AUTHOR(S)**<br>Shaun Eshraghi* (https://orcid.org/0000-0002-8152-0838)<br>Jonathan Gondek** (https://orcid.org/0000-0001-9872-8320)<br>Kris Severson* (https://orcid.org/0000-0002-1039-554X) | **5d. PROJECT NUMBER**<br>RR28A400 |
| | **5e. TASK NUMBER**<br>TJ2C6 |
| | **5f. WORK UNIT NUMBER** |
| **7. PERFORMING ORGANIZATION NAME(S) AND ADDRESS(ES)**<br>*Volpe National Transportation Systems Center, 55 Broadway, Cambridge, MA 02142<br>**Calspan Corporation, 4455 Genesee St, Cheektowaga, NY 14225 | **8. PERFORMING ORGANIZATION REPORT NUMBER** |
| **9. SPONSORING/MONITORING AGENCY NAME(S) AND ADDRESS(ES)**<br>U.S. Department of Transportation<br>Federal Railroad Administration<br>Office of Railroad Policy and Development<br>Office of Research, Development, and Technology<br>Washington, DC 20590 | **10. SPONSOR/MONITOR'S ACRONYM(S)** |
| | **11. SPONSOR/MONITOR'S REPORT NUMBER(S)**<br>DOT/FRA/ORD-21/08 |

**12. DISTRIBUTION/AVAILABILITY STATEMENT**
This document is available to the public through the FRA website at https://railroads.dot.gov/elibrary-search.

**13. SUPPLEMENTARY NOTES**
COR: Kristine Severson (Volpe), Jeffrey Gordon (FRA)

**14. ABSTRACT**
FRA sponsors ongoing research on passenger rail equipment occupant protection at the Volpe Center. The Volpe Center contracted Calspan to conduct pendulum impact testing of the THOR-50M ATD. A series of 28 pendulum impact tests was performed on the lower chest and abdomen of the THOR-50M to evaluate: (1) biofidelity, (2) height sensitivity, (3) velocity sensitivity, and (4) repeatability. The test results indicate that the THOR-50M had a similar level of abdomen biofidelity to other advanced frontal impact ATDs. The THOR-50M was sensitive to variations in impact height and speed, and the tests were generally repeatable. The results will be used to inform potential updates to the abdomen compression performance limit for the THOR-50M in the industry safety standard for crashworthy workstation tables in passenger trains.

**15. SUBJECT TERMS**
Passenger railcar, workstation tables, energy absorption, interior crashworthiness, injury criteria, abdomen injury, anthropomorphic test device, ATD, THOR-50M ATD, train collision safety.

| **16. SECURITY CLASSIFICATION OF:** | | | **17. LIMITATION OF ABSTRACT** | **18. NUMBER OF PAGES** | **19a. NAME OF RESPONSIBLE PERSON** |
|---|---|---|---|---|---|
| **a. REPORT** | **b. ABSTRACT** | **c. THIS PAGE** | | | Jeffrey Gordon |
| Unclassified | Unclassified | Unclassifie d | | 61 | **19b. TELEPHONE NUMBER** *(Include area code)*<br>617-494-2303 |

# METRIC/ENGLISH CONVERSION FACTORS

| ENGLISH TO METRIC | | | METRIC TO ENGLISH | | |
|---|---|---|---|---|---|
| **LENGTH** (APPROXIMATE) | | | **LENGTH** (APPROXIMATE) | | |
| 1 inch (in) | = | 2.5 centimeters (cm) | 1 millimeter (mm) | = | 0.04 inch (in) |
| 1 foot (ft) | = | 30 centimeters (cm) | 1 centimeter (cm) | = | 0.4 inch (in) |
| 1 yard (yd) | = | 0.9 meter (m) | 1 meter (m) | = | 3.3 feet (ft) |
| 1 mile (mi) | = | 1.6 kilometers (km) | 1 meter (m) | = | 1.1 yards (yd) |
| | | | 1 kilometer (km) | = | 0.6 mile (mi) |
| **AREA** (APPROXIMATE) | | | **AREA** (APPROXIMATE) | | |
| 1 square inch (sq in, in$^2$) | = | 6.5 square centimeters (cm$^2$) | 1 square centimeter (cm$^2$) | = | 0.16 square inch (sq in, in$^2$) |
| 1 square foot (sq ft, ft$^2$) | = | 0.09 square meter (m$^2$) | 1 square meter (m$^2$) | = | 1.2 square yards (sq yd, yd$^2$) |
| 1 square yard (sq yd, yd$^2$) | = | 0.8 square meter (m$^2$) | 1 square kilometer (km$^2$) | = | 0.4 square mile (sq mi, mi$^2$) |
| 1 square mile (sq mi, mi$^2$) | = | 2.6 square kilometers (km$^2$) | 10,000 square meters (m$^2$) | = | 1 hectare (ha) = 2.5 acres |
| 1 acre = 0.4 hectare (he) | = | 4,000 square meters (m$^2$) | | | |
| **MASS - WEIGHT** (APPROXIMATE) | | | **MASS - WEIGHT** (APPROXIMATE) | | |
| 1 ounce (oz) | = | 28 grams (gm) | 1 gram (gm) | = | 0.036 ounce (oz) |
| 1 pound (lb) | = | 0.45 kilogram (kg) | 1 kilogram (kg) | = | 2.2 pounds (lb) |
| 1 short ton = 2,000 pounds (lb) | = | 0.9 tonne (t) | 1 tonne (t) | = | 1,000 kilograms (kg) |
| | | | | = | 1.1 short tons |
| **VOLUME** (APPROXIMATE) | | | **VOLUME** (APPROXIMATE) | | |
| 1 teaspoon (tsp) | = | 5 milliliters (ml) | 1 milliliter (ml) | = | 0.03 fluid ounce (fl oz) |
| 1 tablespoon (tbsp) | = | 15 milliliters (ml) | 1 liter (l) | = | 2.1 pints (pt) |
| 1 fluid ounce (fl oz) | = | 30 milliliters (ml) | 1 liter (l) | = | 1.06 quarts (qt) |
| 1 cup (c) | = | 0.24 liter (l) | 1 liter (l) | = | 0.26 gallon (gal) |
| 1 pint (pt) | = | 0.47 liter (l) | | | |
| 1 quart (qt) | = | 0.96 liter (l) | | | |
| 1 gallon (gal) | = | 3.8 liters (l) | | | |
| 1 cubic foot (cu ft, ft$^3$) | = | 0.03 cubic meter (m$^3$) | 1 cubic meter (m$^3$) | = | 36 cubic feet (cu ft, ft$^3$) |
| 1 cubic yard (cu yd, yd$^3$) | = | 0.76 cubic meter (m$^3$) | 1 cubic meter (m$^3$) | = | 1.3 cubic yards (cu yd, yd$^3$) |
| **TEMPERATURE** (EXACT) | | | **TEMPERATURE** (EXACT) | | |
| [(x-32)(5/9)] °F | = | y °C | [(9/5) y + 32] °C | = | x °F |

## QUICK INCH - CENTIMETER LENGTH CONVERSION

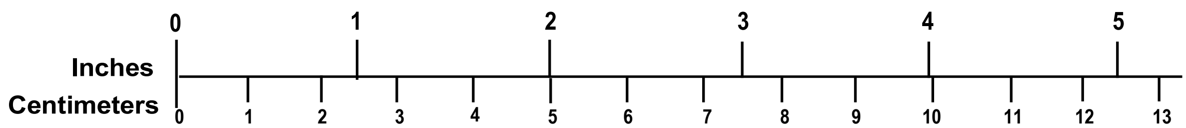


## QUICK FAHRENHEIT - CELSIUS TEMPERATURE CONVERSIO

| | | | | | | | | | | | | | | |
|---|---|---|---|---|---|---|---|---|---|---|---|---|---|---|
| °F | -40° | -22° | -4° | 14° | 32° | 50° | 68° | 86° | 104° | 122° | 140° | 158° | 176° | 194° | 212° |
| °C | -40° | -30° | -20° | -10° | 0° | 10° | 20° | 30° | 40° | 50° | 60° | 70° | 80° | 90° | 100° |

For more exact and or other conversion factors, see NIST Miscellaneous Publication 286, Units of Weights and Measures. Price $2.50 SD Catalog No. C13 10286

Updated 6/17/98

# Contents

## Illustrations

## Tables

## Executive Summary

The THOR 50th Percentile Male (THOR-50M) is an advanced frontal impact anthropomorphic test device (ATD, or crash test dummy). The THOR-50M is designed to have anthropometry similar to a 50th percentile adult male and to respond to impacts in a similar manner. THOR-50M has instrumentation in the head, chest, abdomen, and legs which can measure displacements, forces, and accelerations that can be used to estimate the level of injury that would be suffered by a human occupant.

The Federal Railroad Administration (FRA) Office of Research, Development, and Technology has an ongoing research program on rail equipment crashworthiness which includes a task on occupant protection for passenger equipment. The Volpe National Transportation Systems Center (Volpe Center) has supported the FRA's research program for a number of years. The results from the research program have been used by the American Public Transportation Association (APTA) Passenger Rail (PR) Construction and Structural (CS) Working Group to develop an industry safety standard (APTA-PR-CS-S-018-13) for fixed workstation tables in passenger railcars. This safety standard references the THOR, but does not specify which version. Significant upgrades to the design of the THOR since the publication of the original FRA research [1], which used a THOR-NT, have warranted a research effort to evaluate the lower chest and abdomen of the newer model, the THOR-50M.

The Volpe Center contracted Calspan Corp. to conduct high-energy pendulum impact testing of the THOR-50M at its ATD test laboratory in Buffalo, New York. Researchers performed a series of 28 pendulum impact tests on the lower chest and abdomen of the THOR-50M to evaluate: (1) biofidelity, (2) height sensitivity, (3) velocity sensitivity, and (4) repeatability. The test results indicate that the THOR-50M had a similar level of abdomen biofidelity to other advanced frontal impact ATDs. The THOR-50M was sensitive to variations in impact height and speed, i.e., it responded to different impact conditions. Lastly, the tests were generally repeatable.

While the results indicate that the external abdomen deflection measurements were similar to those measured on the H3-RS and THOR-NT ATDs under the same test conditions, the differences in the internal abdomen deflection measurements between the three ATDs suggest that a performance limit different from that used for the THOR-NT and H3-RS is likely warranted for the THOR-50M for this criterion.

The results of this THOR-50M pendulum test series will be used to inform technical discussions within the APTA PR CS Working Group to inform future revisions to the APTA safety standard. Specifically, the results will be used in discussions on potential updates to the abdomen compression performance limit for the THOR-50M due to an upgrade to the abdomen deflection sensors.

# 1. Introduction

This report documents impact testing of the lower chest and abdomen of an anthropomorphic test device (ATD) – the THOR-50M – using a pendulum equipped with a rigid, round bar impactor (Figure 1). The diameter of the impactor, mass and speed of the pendulum, and height of the impact were varied to evaluate the response of the ATD across a range of impact conditions. The test results will be used by the Federal Railroad Administration (FRA) and the Volpe National Transportation Systems Center (Volpe Center) in technical discussions with industry stakeholders to potentially revise safety performance limits in the industry safety standard for fixed workstation tables in passenger railcars (APTA PR-CS-S-018) [2].

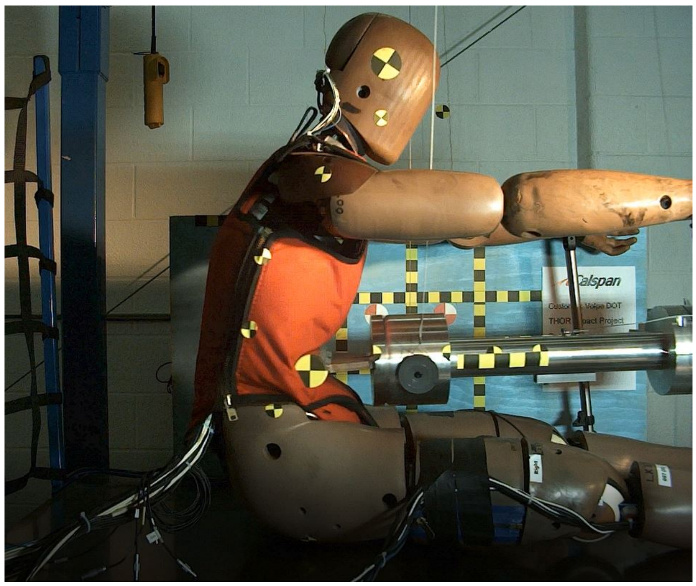


**Figure 1. Abdomen Impact Test of THOR-50M with 2-inch Round Bar Pendulum Impactor**

## 1.1 Background

The Volpe Center has identified risks associated with passengers seated at thin, rigid workstation tables during train accidents [3, 4]. When workstation tables are designed with crashworthy features, they can effectively compartmentalize occupants during collisions and limit concentrated loads on an occupant's chest and abdomen. The APTA safety standard defines performance limits for workstation tables in passenger trains in the U.S., including injury criteria for the head, neck, chest, abdomen, and femurs. To demonstrate compliance with the safety standard, a dynamic sled test is required. The sled test can be conducted per Option A of the standard using either a Hybrid-III Rail Safety ATD (H3-RS) [5] or a THOR ATD with an 8g, 250 ms triangular crash pulse. Option B of the standard allows use of conventional Hybrid-III 50$^{th}$ percentile male (H3-50M) ATDs in all seat positions but requires an additional quasi-static test because the H3-50M cannot measure abdomen deflection.

While the most widely used frontal impact ATD is the H3-50M, it features only a single internal deflection sensor in the chest (located behind the sternum) and no deflection sensors in the abdomen. Low workstation tables do not impact the H3-50M near the sternum, limiting the ability to predict injury with this ATD. In Option A, the workstation table safety standard requires that either the H3-RS or THOR be seated next to the wall, while a standard H3-50M can be placed in other seat positions. An H3-RS or THOR is required in the wall seat because ATDs in that seat position typically experience higher contact forces with the table.

The H3-RS was developed by the Rail Safety Standards Board (RSSB) and the Transport Research Laboratory (TRL) in the U.K. to evaluate thoracic injuries that occur when passengers impact workstation tables during train accidents. The THOR was developed by the National Highway Traffic Safety Administration (NHTSA) to evaluate thoracic injuries that occur when occupants in an automobile impact the steering column, seat belts, or airbag during an automotive accident. Both of the advanced frontal impact ATDs include additional instrumentation to measure deflection and rate of deflection at multiple bilateral locations in the chest and abdomen in order to evaluate injury to the chest and abdomen as a result of different load applications. The H3-RS was designed to meet the certification requirements defined for the THOR in the GESAC[1] 2005.2 THOR Certification Manual [6], which corresponds to an early version of the THOR – referred to as THOR-NT.

Both the H3-RS and THOR have been used to assess injuries in crash tests with fixed workstation tables in passenger rail vehicles. The ATDs are suitable for evaluating injuries from impacts with fixed workstation tables because of their ability to accurately measure internal deflections in the lower chest and abdomen – the regions directly impacted by the leading edge of a table.

FRA conducted a series of full-scale crash tests with a H3-RS and THOR-NT seated facing a rigid table [7] and energy-absorbing (crashworthy) table [1]. Following the full-scale crash tests, a literature review and computational study in MADYMO were performed to determine appropriate injury criteria for a crash test with a crashworthy table [8]. These studies were used to inform technical discussions within the APTA PR CS Working Group. The working group published the original workstation table safety standard APTA-PR-CS-S-018 in March 2013.

As mentioned above, the standard provides options for testing with a H3-RS ATD or a THOR ATD. The chest and abdomen deflection requirements specified in the APTA table standard (original and Revision 1) are the same for both ATDs, as the H3-RS and THOR-NT have approximately the same behavior under loading from table impacts. Hynd and Carroll demonstrated that the THOR-NT and H3-RS experience similar internal deflections from lower chest and abdomen pendulum impacts at TRL in England [9].

The tests described in this report evaluate the biofidelity and impact sensitivity of the latest version of the THOR, referred to as the THOR-50M, under the same conditions used to evaluate the THOR-NT and H3-RS. Since the THOR-50M has fewer deflection sensors, and in different locations in its abdomen, direct comparison to the THOR-NT and the H3-RS is challenging.

For any ATD, the compression of the abdomen and lower chest of the ATDs can be measured internally or externally. Internal deflection is measured by instrumentation located inside the ATD, while external penetration can be measured by video analysis or calculations from accelerometers on the ATD and impactor.

After the pendulum impact study on the H3-RS was completed at TRL, Hynd and Willis evaluated the H3-RS in a series of sled tests with donated crashworthy workstation tables at TRL

[1] General Engineering and Systems Analysis Co. (GESAC), Inc., Boonsboro, MD.

[10]. As of this time of writing, FRA is contracting with MGA Research for a similar series of sled tests with a THOR-50M and industry-donated workstation tables at MGA's test lab in Greer, South Carolina. A separate FRA report will present the test results from workstation table sled tests with a THOR-50M.

## 1.2 Objectives

1. Evaluate the biofidelity of the abdomen of the THOR-50M by comparing test results to target corridors defined in the GESAC 2005.1 THOR-NT Biomechanical Response Requirements [11].
2. Characterize the sensitivity of internal measurements from the lower chest and abdomen of the THOR-50M to variations in impact speed.
3. Characterize the sensitivity of internal measurements from the lower chest and abdomen of the THOR-50M to variations in impactor height.
4. Evaluate the repeatability of measurements from the THOR-50M across different impactor shapes, speeds, and heights.

## 1.3 Overall Approach

The Vehicle Research and Test Center (VRTC) Dummy Management Lab at NHTSA loaned a THOR-50M ATD (Serial #7) to Calspan, a crash test laboratory in Buffalo, New York, for abdomen impact testing. Calspan's ATD laboratory performed the tests with its pendulum impact system equipped with a rigid, round bar impactor having a diameter of 25 mm or 50 mm and a length of 30 cm. Calspan conducted these tests under a contract with the Volpe Center and followed the methodology in the Abdomen Qualification test procedure in Section 9 of the THOR-50M Qualification Manual from August 2016 [12].

## 1.4 Scope

This report describes high-energy pendulum impact testing of the lower chest and abdomen of a THOR-50M. The pendulum impact conditions were chosen to be similar to tests performed by Hynd on the H3-RS [9] so that comparisons could be made between the ATD abdomen responses. This report does not make direct comparisons between the ATDs because it is intended to be a standalone study focusing on the THOR-50M. A follow-on paper will focus on comparing the abdominal response of the THOR-50M and H3-RS.

## 1.5 Organization of the Report

- **Section 2 – Methodology** details the procedures used to conduct the pendulum impact testing, including details on video and data processing, pendulum impact test conditions, and computation of injury criteria.
- **Section 3 – Results and Discussion** presents the key findings of the test program, with a primary focus on the abdomen injury criteria specified in APTA PR-CS-S-018.
- **Section 4 – Conclusion** ends the main body of the report and summarizes the takeaways from the results and how they can be applied to improve passenger rail safety.

## 2. Methodology

Tests were conducted at in the ATD laboratory of Calspan in Buffalo, New York. Calspan has decades of experience performing pendulum impact tests on ATDs for certification to support its vehicle crash and sled testing laboratories. This section describes:

1. Data acquisition and processing
2. High-speed video analysis
3. Test configurations
4. Injury criteria
5. Biofidelity

### 2.1 Data Acquisition and Processing

All instrumentation data channels were programmed and captured using Kistler Data Acquisition Software (DAS) at 20 kHz and processed using National Instruments (NI) DIAdem data processing software. Table 1 summarizes the instrumentation and the channel frequency class (CFC) filters used. All of the deflection sensors in the chest and abdomen are Infra-Red Telescoping Rod for the Assessment of Chest Compression (IR-TRACC) sensors.

**Table 1. Summary of Sensors for Data Acquisition**

| Measurement | Test Article | Sensor Description | Filter(s) |
|---|---|---|---|
| Velocity | Pendulum | Impact X-Velocity Light Trap | N/A |
| Acceleration | Pendulum | Trailing End<br>X,Y,Z Accelerometers | CFC-180 |
| | THOR-50M | T1 Spine<br>X Accelerometer | CFC-1000 |
| | THOR-50M | T6 Spine (Thorax CG Height)<br>X,Y,Z Accelerometers | CFC-1000 |
| | THOR-50M | T12 Spine<br>X,Y,Z Accelerometers | CFC-1000 |
| | THOR-50M | Pelvis<br>X, Y, Z Accelerometers | CFC-1000 |
| Displacement | THOR-50M | Left / Right; Upper / Lower,<br>Chest IR-TRACCs | CFC-600<br>CFC-180 |
| | THOR-50M | Left / Right,<br>Abdomen IR-TRACCs | CFC-600<br>CFC-180 |

Calspan's speed trap system has a constant sampling rate regardless of the speed of the pendulum. This means that the faster the probe travels through the speed trap, the less accurate the probe speed measurement is. An average accuracy of +/- 0.006 m/s was estimated for the range of speeds in this test program, and test speeds are documented at a resolution of 0.01 m/s in this report.

For the data acquisition system, an automatic triggering mechanism was used to determine the time of first contact between the impactor and the ATD. A constant threshold acceleration was used so that time zero corresponded to the first time point where the CFC-180 filtered x-acceleration of the impactor exceeded 1g.

## 2.2 High-speed Video Analysis of External Deflection

High-speed video cameras were positioned to view the impact test from a side view and a front view (at a slightly oblique angle due to the pendulum swing area). Calspan utilized its high-speed cameras and software from Integrated Design Tools (IDT) to post-process the video footage from each impact. The time window for recording high-speed video footage was 50 ms prior to initial impact and 250 ms after initial impact. The frame rate was set at 1,000 frames per second.

For the high-speed video analysis, a triggering mechanism was not used to determine the time of first contact between the impactor and ATD (time zero). The lack of trigger required a manual determination of time zero by the operator inspecting the videos. This was believed to have resulted in test-to-test variability in high-speed video estimations of external deflection.

## 2.3 Test Configurations

A series of impact tests were conducted on the lower chest and abdomen of the THOR-50M. The impactor diameter, pendulum mass, impact velocity, and impact height are specified in this section.

Calspan used a 32-kg pendulum for all impacts except for the velocity sensitivity impacts to the lower chest. A 24-kg pendulum was used for the lower chest velocity sensitivity tests to be closer to what was used for the H3-RS tests [9]. Calspan controlled the impact velocity to target speeds in increments between 3.3 and 7.1 m/s to result in similar kinetic energies as the study on the H3-RS. These targets were chosen to facilitate comparisons between the THOR-50M and H3-RS in future work.

Pendulum mass was controlled to be within ± 0.02 kg of the target mass, and impact velocity was controlled to be within ± 0.05 m/s of the target velocity. Additionally, the left versus right discrepancy in peak x-deflection from the IR-TRACCs closest to the impact height (i.e., having the largest deflections) was required to be less than 12 mm to ensure the THOR-50M was aligned facing the pendulum. These tolerances for the test conditions were specified per the August 2016 THOR-50M Qualification Manual [12]. The tolerances resulted in six re-tests due to the failure to meet the requirements on velocity or left versus right deflection. The re-tests are denoted with a suffix letter starting at "a" after the test number.

Figure 2 shows images of the lower chest and abdomen, with annotations showing the location of the abdomen and lower chest deflection sensors used as reference points to position the height of the impactor. The IR-TRACCs annotated in Figure 2 were positioned at a height near the vertical center of the abdomen and at the anterior attachment of the 6$^{th}$ rib. All IR-TRACCs were symmetric across the left (L) and right (R) sides of the ATD.

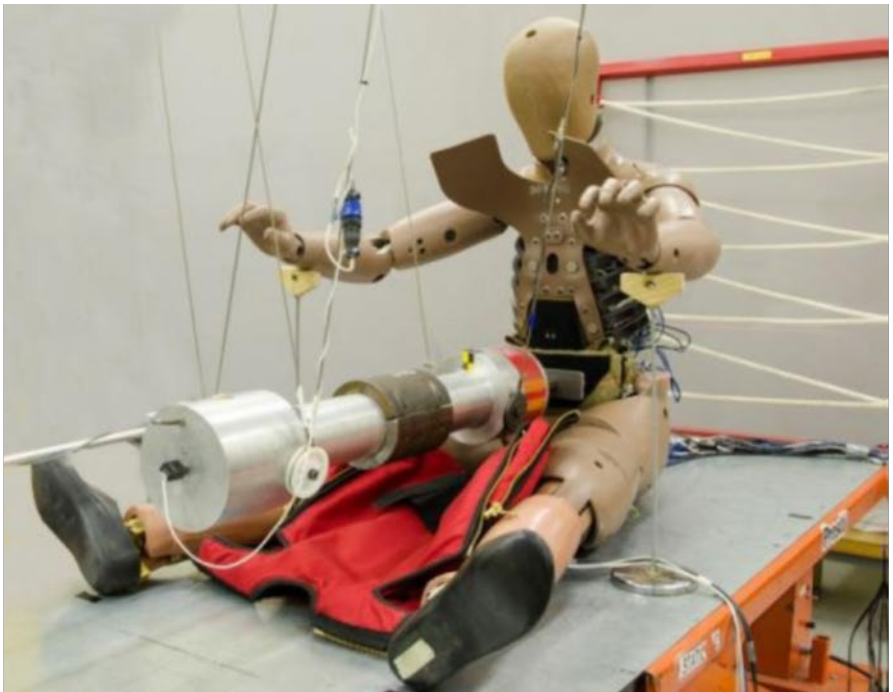

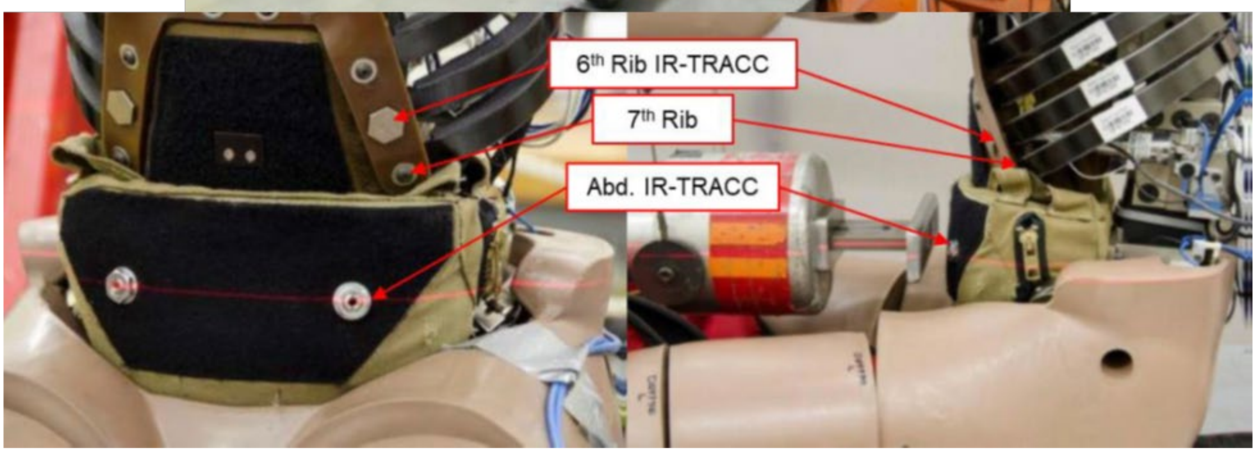


**Figure 2. Images of THOR-50M Depicting Deflection Sensor Locations (THOR-50M 2016 Qualification Manual [12])**

### *2.3.1 Biofidelity Tests – Lower Abdomen with 25-mm-Diameter Round Bar*

Lower abdomen biofidelity tests were conducted using the test conditions described in GESAC 2005.2 with a rigid, 30-cm-long, 25-mm-diameter round bar impactor having a mass of 32 kg at a target speed of 6.1 m/s. The test conditions are provided in Table 2 below.

**Table 2. Conditions for Biofidelity Tests on the Lower Abdomen**

| Category | Impactor | | | | Impact Location | | Repeats |
|---|---|---|---|---|---|---|---|
| | Diameter | Mass | Velocity | KE | Reference Point | Distance | |
| - | *mm* | *kg* | *m/s* | *J* | - | *mm* | # |
| Lower Abdomen Biofidelity | 25 | 32.0 | 6.1 | 595 | Abd. IR-TRACC | 0.0 | 3 |

For all subsequent tests, the diameter of the round bar impactor was increased to 50 mm to be more representative of the leading edge of a crashworthy table in a passenger rail vehicle – following the approach of Hynd [9]. A 25-mm round bar was used for the biofidelity tests in this section so the lower abdomen response could be evaluated using the biofidelity corridors in GESAC 2005.2.

Section 3.1 contains the results of the THOR-50M lower abdomen biofidelity evaluation.

### *2.3.2 Impact Height Sensitivity Tests with 50-mm-Diameter Round Bar*

Five impact points were spaced approximately evenly between the vertical position of the abdomen IR-TRACC and lower chest IR-TRACC (6$^{th}$ rib). The targeted impact heights were spaced approximately 30 mm apart and measured relative to accessible features (reference points) on the anterior surface of the THOR-50M to ensure accurate pendulum positioning relative to the ATD and repeatability between tests. The impact height sensitivity tests had test conditions similar to the lower abdomen biofidelity test, i.e., the target pendulum mass was 32 kg, the target impact velocity was 6.1 m/s, and the impactor was a round bar. However, the impactor diameter increased from 25 mm to 50 mm for the reasons mentioned in the previous section. The height sensitivity test conditions are provided in Table 3 below. For clarification, a reference point at the 7$^{th}$ rib and distance of -28 mm means that the impact occurred 28 mm below the 7$^{th}$ rib.

**Table 3. Conditions for Abdomen Height Sensitivity Tests on the Abdomen**

| Category | Impactor | | | | Impact Location | | Repeats |
|---|---|---|---|---|---|---|---|
| | Diameter | Mass | Velocity | KE | Reference Point | Distance | |
| - | *mm* | *kg* | *m/s* | *J* | - | *mm* | # |
| Height Sensitivity | 50 | 32.0 | 6.1 | 595 | 6$^{th}$ Rib IR-TRACC | 0.0 | 3 |
| Height Sensitivity | 50 | 32.0 | 6.1 | 595 | 7$^{th}$ Rib | 0.0 | 3 |
| Height Sensitivity | 50 | 32.0 | 6.1 | 595 | 7$^{th}$ Rib | -28.0 | 3 |
| Height Sensitivity | 50 | 32.0 | 6.1 | 595 | Abd. IR-TRACC | 38.0 | 3 |

| Category | Impactor | | | | Impact Location | | Repeats |
|---|---|---|---|---|---|---|---|
| | Diameter | Mass | Velocity | KE | Reference Point | Distance | |
| - | *mm* | *kg* | *m/s* | *J* | - | *mm* | # |
| Height Sensitivity | 50 | 32.0 | 6.1 | 595 | Abd. IR-TRACC | 0.0 | 1 |

Repeats were not performed for the lowest impact height (centered on the abdomen IR-TRACC) because it was expected that the 50-mm impactor would interact with the anterior superior iliac spine (ASIS) rigid parts and result in vertical displacement of the impactor. Figure 3 shows the relative position of the impactor (green) and ASIS parts (red). It was not clear whether or not the 25-mm impactor would impact the ASIS parts; it typically depends on the exact positioning of the pelvis.

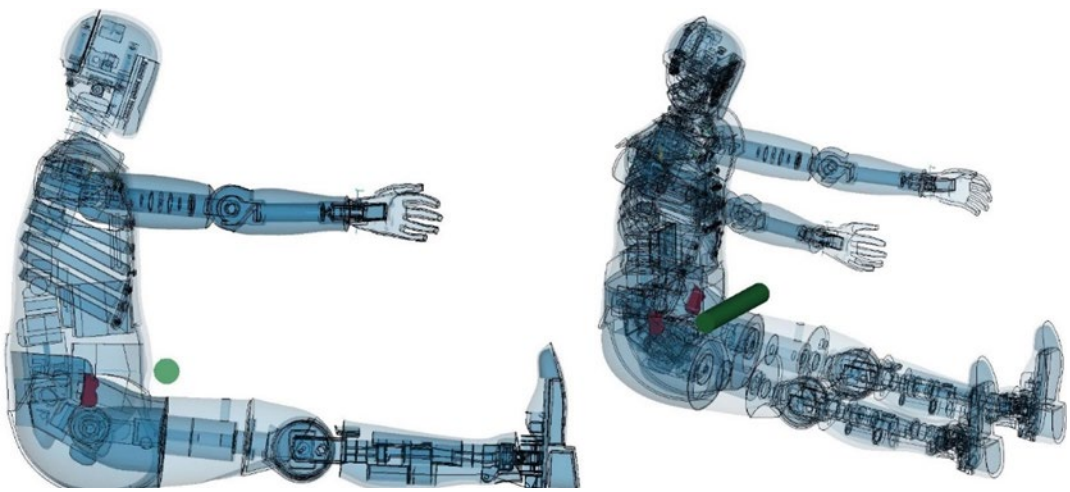

**Figure 3. Views of THOR-50M Finite Element Model showing ASIS Parts in Red and 50-mm Impactor in Green; Impactor Positioned at Height of Abdomen IR-TRACC**

Section 3.2 contains the results of the THOR-50M impact height sensitivity study.

### *2.3.3 Velocity Sensitivity Tests with 50 mm Round Bar*

Two sets of velocity sensitivity tests were specified for impacts to the lower chest and abdomen. The mass of the pendulum was 24 kg for the lower chest and 32 kg for the abdomen. Incremental changes were made to the speed of the pendulum to evaluate the sensitivity of the lower chest and abdomen to changes in impact velocity (also kinetic energy). Impact velocity was controlled to be within ±0.05 m/s of the target velocity. Each test at a given speed had two repeats. The test conditions are provided in Table 4 below.

**Table 4. Conditions for Velocity Sensitivity Tests**

| Category | Impactor | | | | Impact Location | | Repeats |
|---|---|---|---|---|---|---|---|
| | Diameter | Mass | Velocity | KE | Reference Point | Distance | |
| - | *mm* | *kg* | *m/s* | *J* | - | *mm* | # |
| Speed Sensitivity | 50 | 24.0 | 5.0 | 300 | 7th Rib | 0.0 | 2 |
| Speed Sensitivity | 50 | 24.0 | 6.0 | 432 | 7th Rib | 0.0 | 2 |
| Speed Sensitivity | 50 | 24.0 | 7.0 | 588 | 7th Rib | 0.0 | 2 |
| Speed Sensitivity | 50 | 32.0 | 3.3 | 174 | Abd. IR-TRACC | 38.0 | 2 |
| Speed Sensitivity | 50 | 32.0 | 5.2 | 433 | Abd. IR-TRACC | 38.0 | 2 |
| Speed Sensitivity | 50 | 32.0 | 7.1 | 807 | Abd. IR-TRACC | 38.0 | 2 |

Section 3.3 contains the results of the THOR-50M velocity sensitivity studies.

### *2.3.4 Summary of Pendulum Impact Tests*

For convenience, Table 5 provides a summary of the test conditions for all 28 pendulum impact tests.

**Table 5. Full Test Matrix**

| Test Number | | Category | Impactor | | | | Impact Location | | Repeats |
|---|---|---|---|---|---|---|---|---|---|
| start | stop | | Diameter | Mass | Velocity | KE | Reference Point | Distance | |
| # | # | - | *mm* | *kg* | *m/s* | *J* | - | *mm* | # |
| 1 | 3 | Lower Abdomen Biofidelity | 25 | 32.0 | 6.1 | 595 | Abdomen IR-TRACC | 0.0 | 3 |
| 4 | 6 | Height Sensitivity | 50 | 32.0 | 6.1 | 595 | 6th Rib IR-TRACC | 0.0 | 3 |
| 7 | 9 | Height Sensitivity | 50 | 32.0 | 6.1 | 595 | 7th Rib | 0.0 | 3 |
| 10 | 12 | Height Sensitivity | 50 | 32.0 | 6.1 | 595 | 7th Rib | -28.0 | 3 |
| 13 | 15 | Height Sensitivity | 50 | 32.0 | 6.1 | 595 | Abdomen IR-TRACC | 38.0 | 3 |

| Test Number | | Category | Impactor | | | | Impact Location | | Repeats |
|---|---|---|---|---|---|---|---|---|---|
| start | stop | | Diameter | Mass | Velocity | KE | Reference Point | Distance | |
| # | # | - | *mm* | *kg* | *m/s* | *J* | - | *mm* | # |
| 16 | 16 | Height Sensitivity | 50 | 32.0 | 6.1 | 595 | Abdomen IR-TRACC | 0.0 | 1 |
| 17 | 18 | Speed Sensitivity | 50 | 24.0 | 5.0 | 300 | $7^{th}$ Rib | 0.0 | 2 |
| 19 | 20 | Speed Sensitivity | 50 | 24.0 | 6.0 | 432 | $7^{th}$ Rib | 0.0 | 2 |
| 21 | 22 | Speed Sensitivity | 50 | 24.0 | 7.0 | 588 | $7^{th}$ Rib | 0.0 | 2 |
| 23 | 24 | Speed Sensitivity | 50 | 32.0 | 3.3 | 174 | Abdomen IR-TRACC | 38.0 | 2 |
| 25 | 26 | Speed Sensitivity | 50 | 32.0 | 5.2 | 433 | Abdomen IR-TRACC | 38.0 | 2 |
| 27 | 28 | Speed Sensitivity | 50 | 32.0 | 7.1 | 807 | Abdomen IR-TRACC | 38.0 | 2 |

Appendix A contains a table of peak results from all of the pendulum impact tests.

### 2.4 Injury Criteria

Table 6 provides a summary of the chest and abdomen injury criteria evaluated for the THOR-50M. These include filtering and performance limits for chest deceleration, chest compression, chest viscous criterion (VC), abdomen compression, and abdomen VC.

Calspan captured and processed the following data from all instrumentation noted in prior sections of this document to compute the injury criteria. Test data were processed per the definitions in APTA-PR-CS-S-018, Rev. 1. Test data were filtered following the procedures in SAE Recommended Practice J211/1 [13] and SAE Recommended Practice J1727 [14].

Note that while peak deflections were calculated using IR-TRACC data filtered at CFC-600 per SAE J211/1, peak VCs were calculated using IR-TRACC data filtered at CFC-180 per the recommendations in SAE J1727 to reduce the effect of high-frequency noise on the first derivative of x-deflection, i.e., x-velocity. Appendix D contains additional details regarding the processing of VC.

**Table 6. THOR-50M Chest and Abdomen Injury Criteria Filtering and Performance Limits**

| Injury Criterion | THOR-50M Sensor(s) | APTA S-018, Rev. 1 Performance Limit |
|---|---|---|
| Chest deceleration, 3 ms Resultant | T6 Spine X,Y,Z Accelerometers | 60g |
| Chest compression, X-axis | Left / Right; Upper / Lower, Chest IR-TRACCs | 63 mm |
| Chest VC, X-axis | Left / Right; Upper / Lower, Chest IR-TRACCs | 1.0 m/s |
| Abdomen compression, X-axis | Left / Right, Abdomen IR-TRACCs | 67 mm† |
| Abdomen VC, X-axis | Left / Right, Abdomen IR-TRACCs | 1.98 m/s |

† THOR-50M abdomen compression performance limit is currently under review by APTA CS Working Group for Revision 2 of APTA-PR-CS-S-018-13 standard.

Calspan supplied filtered and raw data files in Microsoft Excel format to the Volpe Center. The Volpe Center then further analyzed the test data and plotted the results in Microsoft Excel for this report.

## 2.5 Biofidelity

The test conditions for the abdomen biofidelity tests are described in Section 2.3.1. The abdomen biofidelity tests were designed to be similar to the lower abdomen tests conducted by Cavanaugh [15] in terms of mass (32 ± 0.02 kg), bar (25-mm diameter, 30-cm long), impact location (~L3, or umbilicus), and velocity (4.9 to 7.2 m/s). The results from Cavanaugh et al. were used to create the biofidelity corridors specified in GESAC 2005.1 THOR Biomechanical Response Requirements.

The upper abdomen biofidelity test specified in GESAC 2005.1 and GESAC 2005.2 is based on work by Nusholtz [16], using a steering wheel-shaped rigid impactor with a mass of 18 kg. Both the lower abdomen and upper abdomen biofidelity tests were conducted on the H3-RS at TRL [9]. However, the upper abdomen biofidelity test could not be performed on the THOR-50M in this test program because the pendulum test system could not safely and controllably achieve the required impact speed (8.0 m/s).

Due to the pendulum speed limitation, the current THOR-50M test program did not use a steering wheel-shaped impactor for any of the tests. Pendulum impacts at the same height (7$^{th}$ rib) and close to the kinetic energy specified in the upper abdomen biofidelity test (576 J) were conducted using a 50-mm round bar. The impact speed was 7.0 m/s and the mass was 24 kg.

Figure 4 shows the lower and upper abdomen biofidelity corridors defined in GESAC 2005.1.

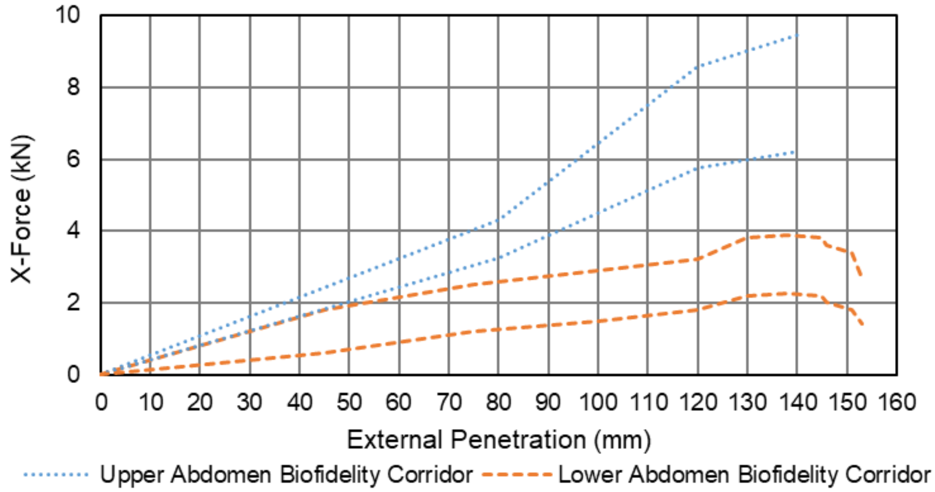


**Figure 4. Lower Abdomen and Upper Abdomen Biofidelity Corridors Defined in GESAC 2005.1 THOR Biomechanical Response Requirements**

Evaluation of the ATD's abdomen biofidelity requires calculation of the external compressive x-deflection (penetration) of the impactor into the abdomen of the ATD. Two methods were used in this test program to estimate penetration: (1) high-speed video analysis and (2) integration of pendulum and T12 spine accelerometers. In general both estimates were in good agreement, and because it is not clear which estimate was more accurate, both are included in this report in plots showing penetration used to evaluate biofidelity.

### *2.5.1 Double Integration Estimate of Abdomen Penetration*

The filtered accelerations from the X accelerometers on the pendulum and T12 spine were both integrated once to calculate change in x-velocity. To calculate the pendulum's x-velocity relative to the THOR-50M, the change in x-velocity was offset by the initial x-velocity measured by the speed trap. Both the T12 and pendulum x-velocities were then integrated again to calculate absolute x-displacement. Finally, the difference between the pendulum x-displacement and the T12 x-displacement was used as an estimate of penetration.

While this procedure was followed using filtered x-accelerations from the T1, T6, T12, and pelvis accelerometers, the T12 accelerometer always resulted in the largest estimate of ATD abdomen penetration likely because it was closest to the impact height. The locations of the accelerometers are shown in a side view of the THOR-50M FE model in Figure 5.

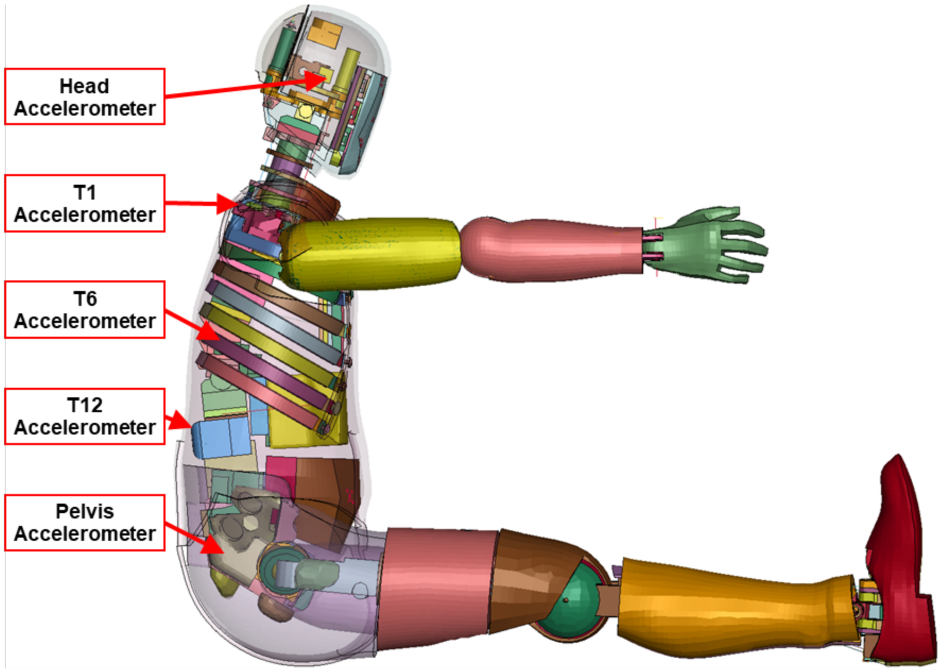


**Figure 5. Annotated Locations of Accelerometers in THOR-50M FE Model**

### *2.5.2 High-Speed Video Estimate of Abdomen Penetration*

Reference measurements were taken with the high-speed side view camera before each impact to post-process penetration of the impactor from each frame of the 1,000 fps videos. Figure 6 shows a still frame taken from the side view camera with annotations for the targets used for displacement measurements.

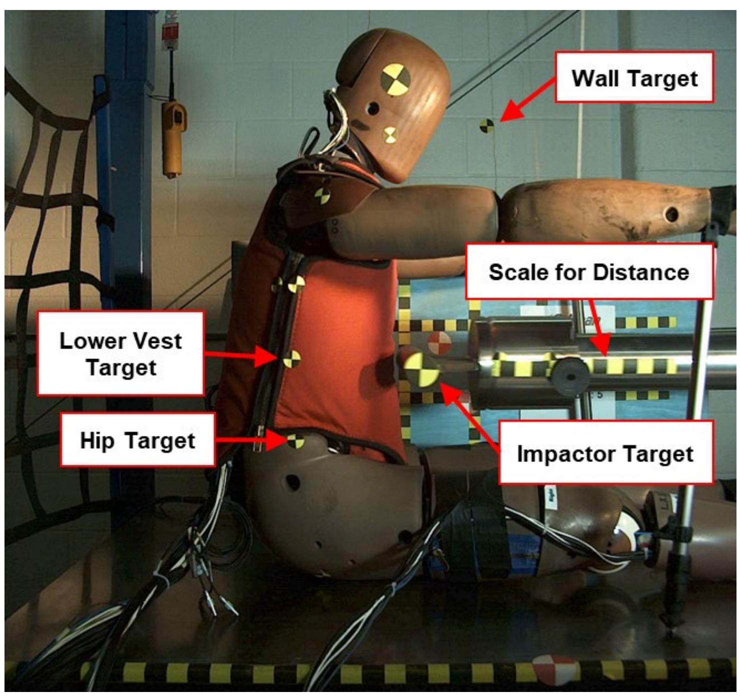


**Figure 6. Annotated Pendulum Impact Test Setup**

Horizontal (X) and vertical (Y) distance measurements were taken from the *Wall Target* to the *Lower Vest Target* and *Hip Target* on the THOR-50M and the *Impactor Target* on the pendulum. The *Wall Target* acted as a static reference to calculate relative distances. The X and Y distances from the *Impactor Target* were subtracted from the X and Y distances from the *Lower Vest Target* and *Hip Target*. These relative distances were then zeroed at the point of contact between the impactor and the THOR-50M so that they estimated the external penetration of the impactor into the abdomen of the ATD.

While either the *Lower Vest Target* or *Hip Target* could be used to estimate external penetration, only the ATD target that resulted in a lower estimate for penetration is documented in this report. This is because the ATD target which resulted in a lower estimate of penetration was always closer to the impact height and therefore a better reference point. A similar approach was used by Cavanaugh [15].

# 3. Results and Discussion

High-speed test videos and reports have been made publicly available in NHTSA's Biomechanics Test Database [17] for each of the pendulum impact tests. These reports and videos were provided to NHTSA by Calspan to fulfill one of the terms in the loan agreement for the THOR-50M ATD. The database includes tests that were repeated due to left versus right discrepancies in IR-TRACC measurements or measured pendulum speeds that were not within tolerance for the target impact speed. The pendulum impact tests described in this report correspond to *Test Number* 12991 through 13023 in the Biomechanics Test Database. The *Reference Number* field in the database corresponds to the test number (Test 1 to 28b) in this report. A letter after the test number denotes a test that was redone to meet the tolerances on the impact conditions taken from the THOR-50M Qualification Manual from August 2016 [12].

## 3.1 Lower Abdomen Biofidelity Tests

Evaluation of the lower abdomen biofidelity of an ATD is intended to characterize how human-like the stiffness the abdomen test device of the ATD is. A more human-like ATD is a better predictor of injuries that would be suffered by a real human occupant in a crash scenario.

A range of force-penetration responses were observed by Cavanaugh during human cadaver testing [15], and the biofidelity corridor proposed in GESAC 2005.1 is intended to bound the typical response of a 50th percentile adult male. This report describes the lower abdomen biofidelity test conditions in Section 2.3.1.

### *3.1.1 External Abdomen Deflection*

Figure 7 shows the lower abdomen biofidelity corridor specified in GESAC 2005.1 and the force versus penetration response of the THOR-50M. Force is calculated as the mass of the pendulum multiplied by the x-acceleration of the pendulum. Penetration was estimated by double integration of x-acceleration (refer to Section 2.5.1). The THOR-50M appeared to exit the biofidelity corridor after 85–90 mm of penetration. The same biofidelity corridor exit range was reported for the THOR-NT (refer to Section 12.2 of GESAC 2005.1) and H3-RS [9]. Two peaks in force were observed in the Test 1 (blue) and Test 2a (orange) curves, while only one peak was observed in the Test 3 (green) curve. This was attributed to a glancing impact between the rigid ASIS parts and the 25-mm impactor (a 50-mm impactor is shown in Figure 3).

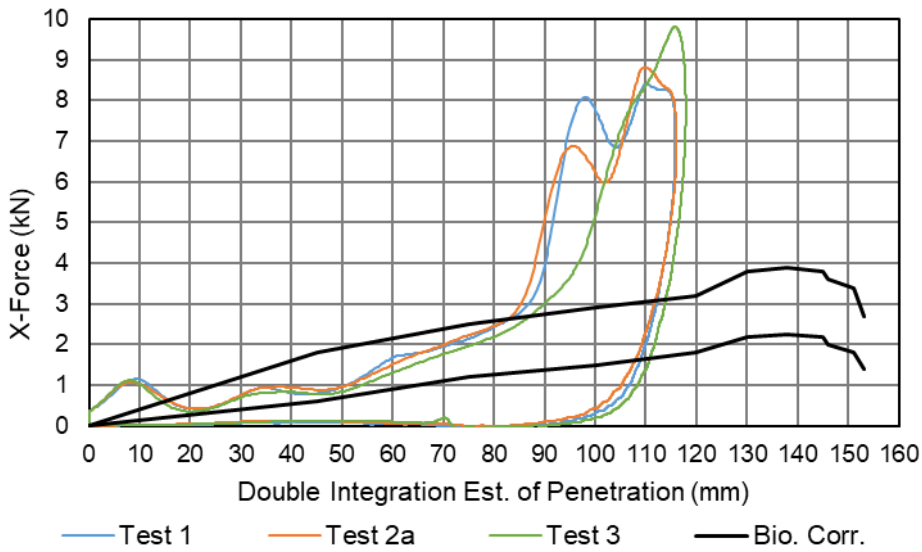


**Figure 7. Lower Abdomen Biofidelity Tests – Pendulum X-Force vs. Double Integration Estimate of Penetration (CFC-180 Force and Accelerations)**

Figure 8 shows the same GESAC 2005.1 lower abdomen biofidelity corridor, but the THOR-50M force-penetration response was updated to use the high-speed video estimation for external penetration (refer to Section 2.5.2). The biofidelity corridor exit range was 95–110 mm using this estimation of external penetration. A large amount of variability can be seen when using the video estimation of penetration, attributable to the interaction between the pendulum and ASIS parts (as discussed in Section 2.3.2) and difficulty in determining the point of contact (time zero) between the impactor and ATD (as discussed in Section 2.2).

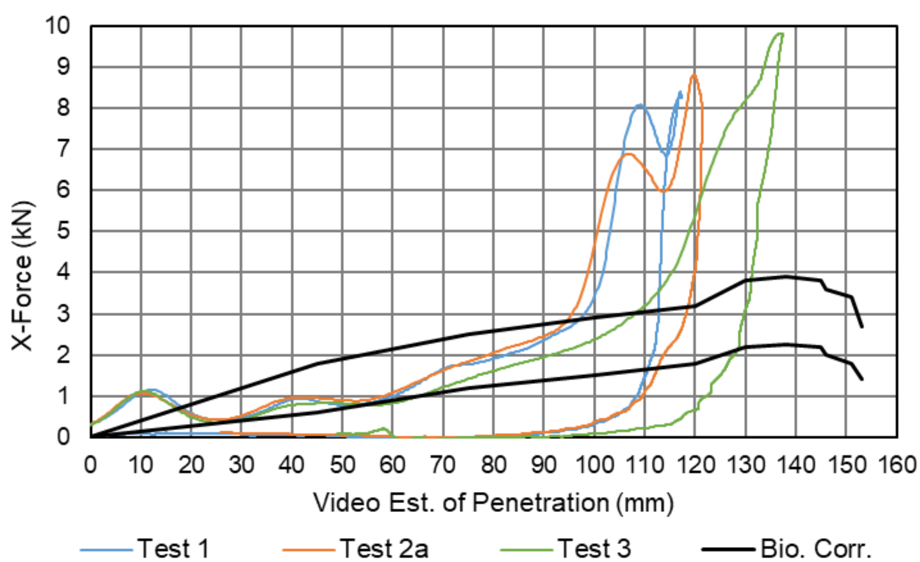


**Figure 8. Lower Abdomen Biofidelity Tests – Pendulum X-Force vs. High-Speed Video Estimate of Penetration (CFC-180 Force, Unfiltered External Penetration)**

The procedure used in GESAC 2005.1 to estimate external penetration of the THOR-NT was unknown. If penetration is estimated by double integration of accelerometer data then it would appear that the THOR-50M stiffness measured externally is unchanged from the THOR-NT. Accurate and repeatable high-speed video analysis is difficult to perform and comparisons between the THOR-NT and THOR-50M lower abdomen biofidelity tests may not be appropriate, using this method.

It is interesting to note that Cavanaugh used both techniques when estimating penetration in human cadavers because the video targets detached during some of the tests [15]. Hynd also experienced problems with video analysis during lower and upper abdomen biofidelity testing of the H3-RS and used the double integration estimation of external penetration [9].

### 3.1.2 Internal (IR-TRACC) Abdomen Deflection

Figure 9 is a plot of three repeats of the lower abdomen biofidelity test (Tests 1–3) showing pendulum x-force versus left (L) and right (R) abdomen IR-TRACC x-deflection. The THOR-NT certification target box from GESAC 2005.1 is also included, and the THOR-NT's certification requires that the force-deflection curve intersect the box while the pendulum is moving into the ATD, i.e., not unloading. It is clear that the target box was not intercepted according to the THOR-50M deflection time-history data. This result indicates that the stiffness of the THOR-50M abdomen (as measured internally) had been reduced since the THOR-NT was upgraded.

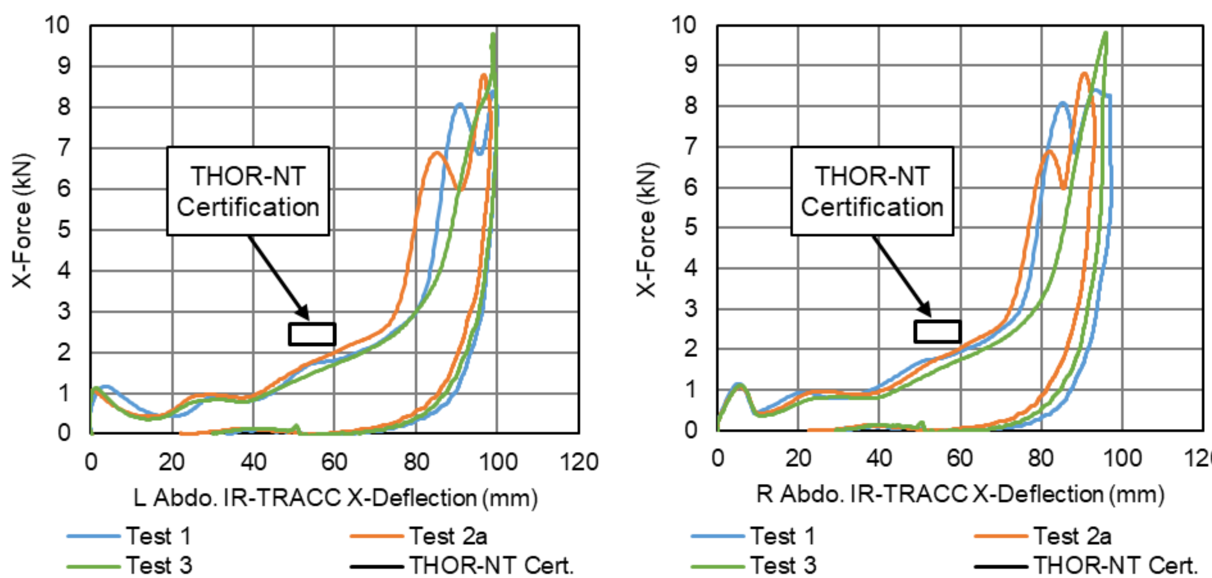


**Figure 9. Lower Abdomen Biofidelity Tests – Pendulum X-Force vs. L (Left) and R (Right) Abdomen IR-TRACC X-Deflection (CFC-180 Force, CFC-600 Deflection)**

Note that the right abdomen IR-TRACC malfunctioned after Test 1. The initial (pre-impact) tube voltage went out of calibration and fluctuated for the remaining tests, making the computed right abdomen IR-TRACC x-deflections and VCs unreliable.

While the materials and design of the abdomen test device (abdomen bag) remained largely unchanged in the incremental upgrades from the THOR-NT to the THOR-50M design, the abdomen deflection sensors were changed from double-gimballed string potentiometers (DGSPs) to IR-TRACCs. Given that DGSPs require pre-tension to operate, it is reasonable to assume that the THOR-NT and H3-RS DGSPs and soft abdomen foam were pre-compressed before being struck by the impactor. The lack of abdomen deflection sensor pre-tension in the THOR-50M could explain the apparent reduction in stiffness observed in Figure 9.

As mentioned in Section 3.1.1, no difference in external penetration was observed when comparing the THOR-NT and THOR-50M, i.e., it was only observed by the internal deflection sensors. The lack of apparent difference externally may have been due to the fact that the sensors measuring internal deflection were laterally offset (left and right) from the centerline of the ATD. While external penetration was measured at the centerline of the ATD, internal deflection was measured at the laterally offset sensor locations – approximately 65 mm away from the centerline. If the pre-compression from the DGSPs was localized in the abdomen foam near the anterior (front) attachment point of each sensor, then pre-compression would not be apparent externally at the centerline of the ATD.

While the authors could not find an image of the THOR-NT showing the pre-compression, the pre-compression was clearly visible in the THOR-Alpha, which also uses DGSPs. Figure 10 shows the pre-compression in the THOR-Alpha abdomen; the photo is from the THOR-Alpha Users' Manual [18].

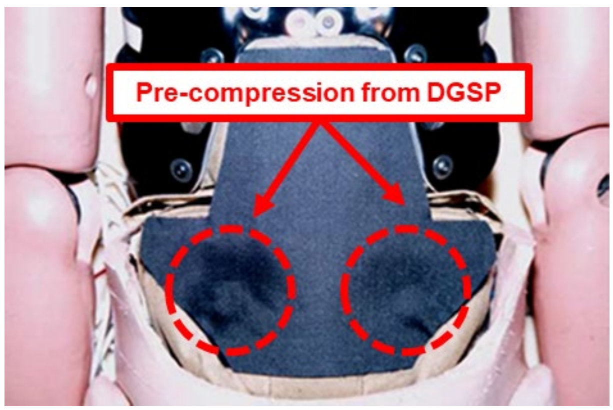


**Figure 10. Photo of THOR-Alpha Abdomen Showing Foam Pre-compression around Abdomen DGSPs (THOR-Alpha Users' Manual [18])**

## 3.2 Impact Height Sensitivity Tests

The impact height sensitivity of the THOR-50M is important to characterize in order to understand how it would deform due to impacts from passenger rail workstation tables, which can be positioned at various heights relative to occupants. It was expected that vertical positions on the ATD which result in large penetrations would tend to be associated with more severe injuries. Crashworthy table systems positioned near the soft regions of the ATD will likely need to limit contact forces to a greater degree in order to prevent injury.

Appendix B contains additional results from the height sensitivity tests.

### *3.2.1 Force-Penetration*

Figure 11 shows force versus external penetration results at various impact heights between the $6^{th}$ rib IR-TRACCs (0 mm) and the abdomen IR-TRACCs (-125 mm). A general trend of increasing peak force and penetration was observed as the impact height was lowered. When the pendulum impacted the ribs, it was clear that a lower penetration occurs because the ribs were stiffer. When the pendulum impacted the abdomen, a higher peak force occurred because the abdomen was initially much softer and then exhibited an abrupt increase in stiffness and force when the abdomen foams fully compressed.

The impacts to the upper abdomen (-59 mm) and middle abdomen (-87 mm) resulted in similar force-penetration curves shown in yellow and orange. At the lowest height (-125 mm) corresponding to the abdomen IR-TRACCs, the 50-mm round bar impactor appeared to interact with the ASIS load cells and resulted in a noticeably different force-penetration curve shape, with a large peak force (~11 kN) at a penetration of ~103 mm. The interaction with the ASIS load cells was expected at the lowest impact height which is why only a single test was performed at -125 mm, while three identical tests were performed at the other heights.

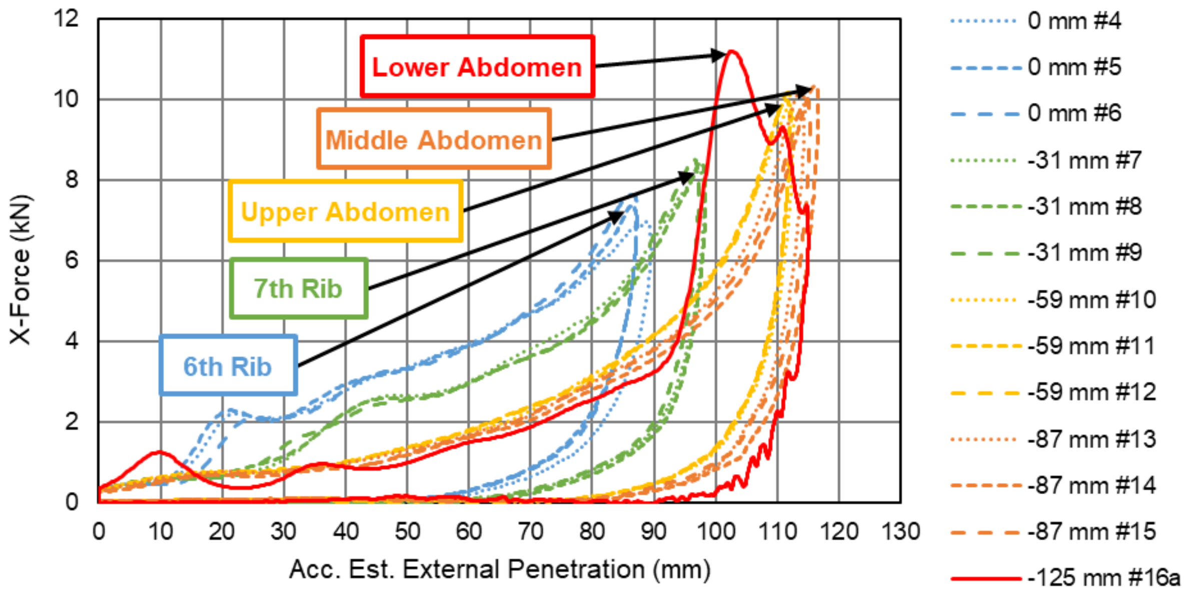


**Figure 11. Impact Height Sensitivity Tests – Pendulum X-Force vs. External Penetration (Accelerometer Estimate) for Impact Heights 0 to 125 mm below 6th Rib (CFC-180 Force and Acceleration)**

### *3.2.2 Peak Compression*

Figure 12 shows peak external penetration (measured by video and accelerometer) versus impact height relative to the lower chest IR-TRACC on the 6th rib. The peak values were taken from the time history data shown in Figure 11. The penetration results showed a significant height sensitivity between the abdomen and the 7th rib. This result was expected, as the abdomen bag is filled with a soft foam, while the ribs are comparatively stiffer.

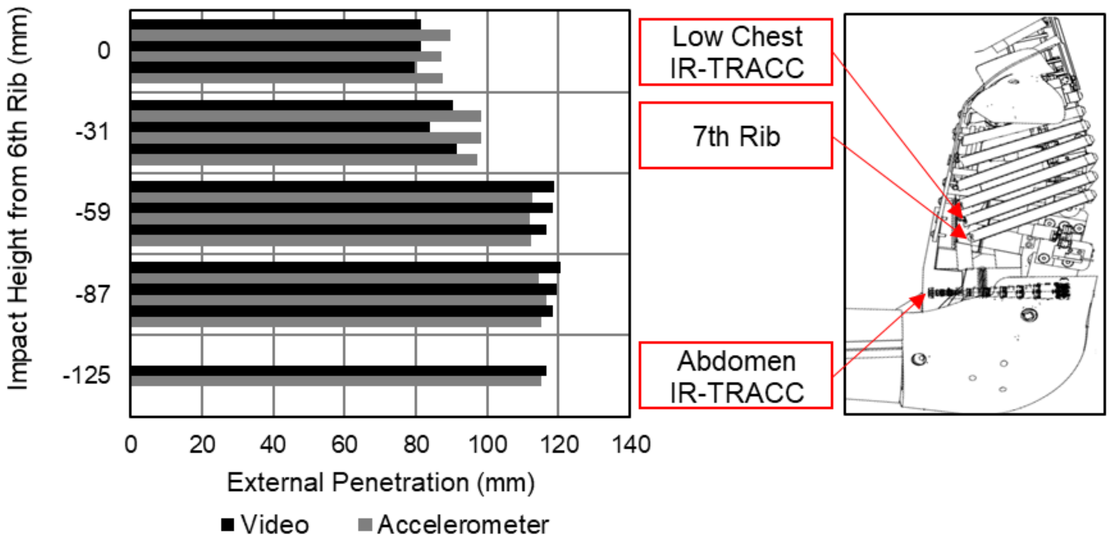


**Figure 12. Impact Height Sensitivity Tests – Peak External Penetration with a 6.1-m/s, 32-kg, 50-mm Round Bar Impactor (CFC-180 Accelerations)**

Figure 13 shows the height sensitivity of peak internal x-deflection measured by the IR-TRACCs. The plot shows the average (left and right) of the IR-TRACC set (lower chest or abdomen) which recorded the highest peak deflection. The average was normalized by the corresponding external penetration measurement shown in Figure 12. Ideally the values would be fairly constant if the sensors were spaced close enough to measure internal deflection for all impact heights, i.e., no dead-zones were present. However, the normalized IR-TRACC x-deflections were reduced at the height of the 7th rib compared to the 6th rib. Also, the peak internal deflections were reduced in the middle and upper abdomen areas (59 mm and 87 mm below the 6th rib) compared to the lower abdomen (125 mm below the 6th rib).

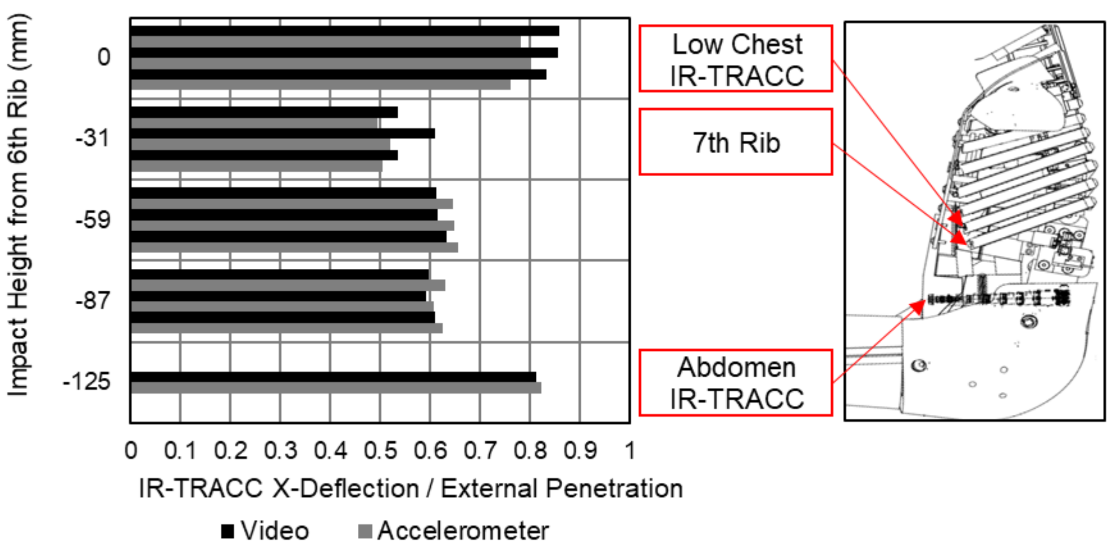


**Figure 13. Impact Height Sensitivity of Peak Internal (IR-TRACC) X-deflection Normalized by External Penetration with a 6.1-m/s, 32-kg, 50-mm Round Bar Impactor (CFC-600 Deflections, CFC-180 Accelerations)**

### 3.2.3 Peak Viscous Criterion

Figure 14 shows peak external VC (measured by video and accelerometer) versus impact height relative to the lower chest IR-TRACC on the 6th rib. An unusually high VC was estimated by video analysis for the lowest impact height – likely due to measurement error. If this extraneous VC measurement is neglected, then the external VC results did not show a significant height sensitivity. This was likely a result of the difference in the equations used to compute chest VC (0 and -31 mm) and abdomen VC (-59, -87, and -125 mm). The equations are presented in Appendix D. The difference in the equations means that for the same measurements of x-deflection and x-velocity in the chest and abdomen, the resulting chest VC would be 43 percent higher than abdomen VC due to the difference in the constants used in the equations (the proportionality factor and undeformed depth).

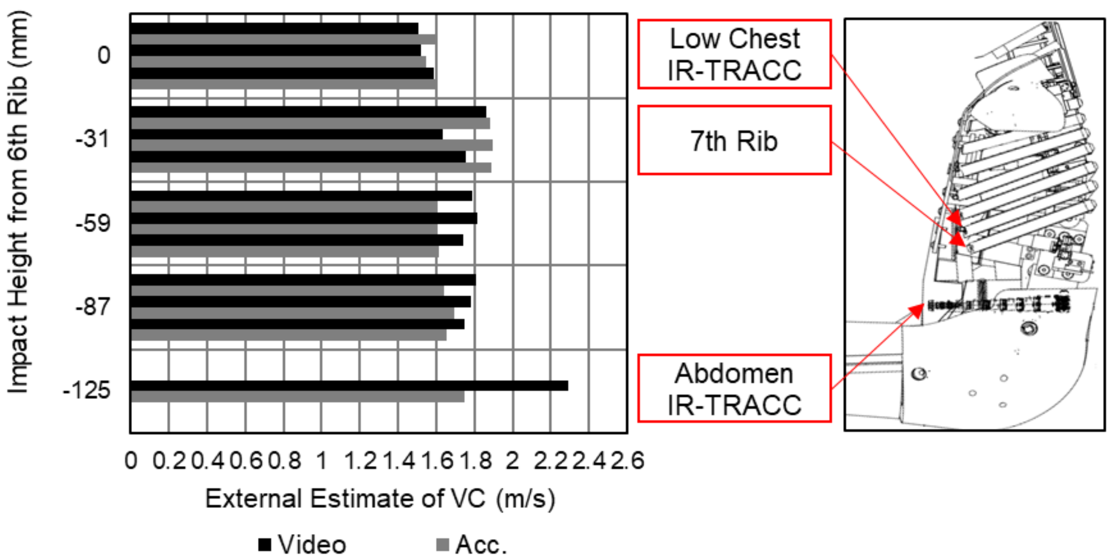


**Figure 14. Impact Height Sensitivity of Peak External Viscous Criterion (Video and Accelerometer Estimates) with a 6.1-m/s, 32-kg, 50-mm Round Bar Impactor (CFC-180 Accelerations)**

Figure 15 shows the height sensitivity of internal VC measured by the IR-TRACCs. The plot shows the average (left and right) of the IR-TRACC set (lower chest or abdomen) which recorded the highest peak VC. The IR-TRACC VC was normalized by the corresponding external VC measurement shown in Figure B5. Ideally, the values would be nearly constant regardless of impact height if the IR-TRACCs were spaced vertically close enough together so that no dead-zones were present. However, as the impactor was moved away from the IR-TRACCs, normalized VC was reduced. The deviation in the peaks shown at a height of -125 mm were due to disagreement between the video and acceleration estimates of external VC visible in Figure 14.

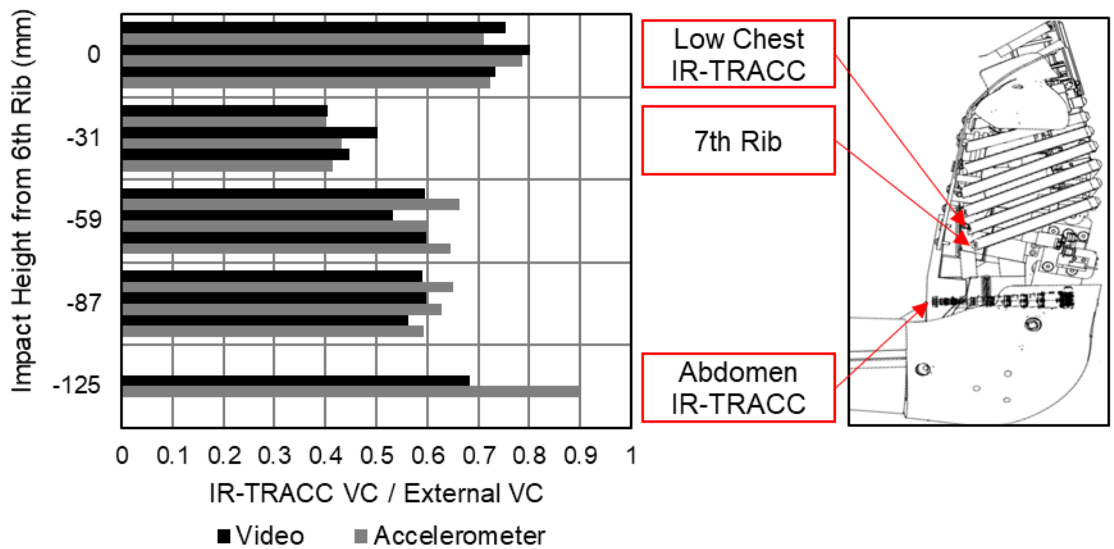


**Figure 15. Impact Height Sensitivity of Peak IR-TRACC Viscous Criterion Normalized by External Viscous Criterion with a 6.1-m/s, 32-kg, 50-mm Round Bar Impactor (CFC-180 Deflections and Accelerations)**

Given that the ribs have similar stiffness, the drop in normalized IR-TRACC VC between the 6th and 7th ribs (see Figure 12) was likely due to the sensor being further from the impact position. While similar pendulum impacts on the H3-RS did not show such a significant height sensitivity for chest VC, the H3-RS was not impacted directly on the lower chest compact rotary unit (CRUX), so the highest value for lower chest VC was not measured in that study [9]. Also, the H3-RS has an upper abdomen deflection sensor in the region where the normalized VC results were low for the THOR-50M, which may have helped lessen the relative change in VC in the upper versus lower abdomen for the H3-RS.

## 3.3 Velocity Sensitivity Tests

Velocity sensitivity tests were conducted on the lower chest and upper abdomen of the THOR-50M to investigate the relationship between impact speed and peak force and deflection and to study rate effects in the shape of the force-displacement response for the two impact regions.

Appendix C contains additional results for the velocity sensitivity tests.

### *3.3.1 Lower Chest Sensitivity Tests*

Figure 16 shows pendulum x-force versus external penetration (estimated by accelerometers) from impacts to the lower chest at target speeds of 5, 6, and 7 m/s. Two tests were performed at each speed. Peak force and external penetration increased as the impact speed increased. The force-penetration results from the different speeds generally followed the same loading curve, except that the 6 m/s tests showed an increase in stiffness after 80 mm of penetration.

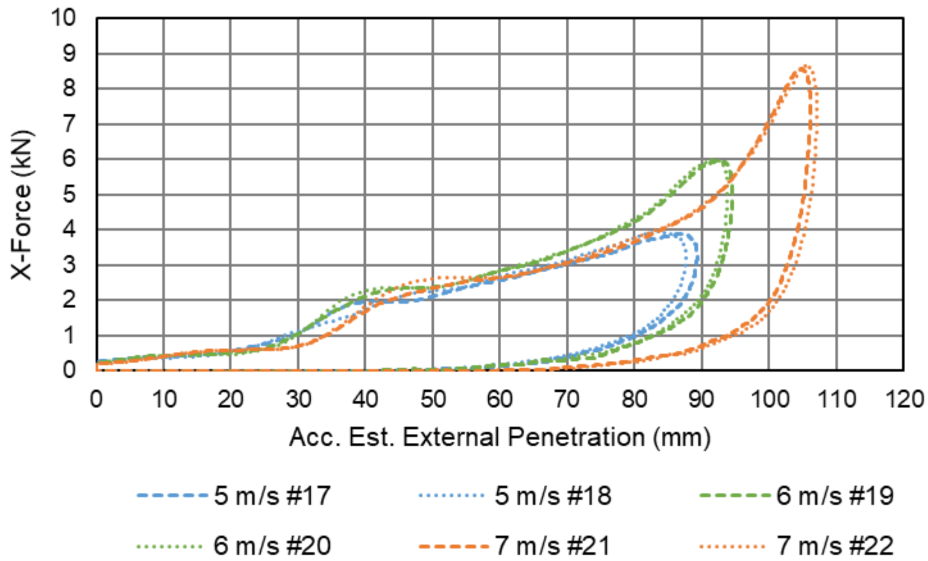


**Figure 16. Lower Chest Velocity Sensitivity Tests – Pendulum X-Force vs External Penetration with a 24-kg, 50-mm round bar (CFC-180 Accelerations and Forces)**

Figure 17 shows pendulum x-force versus left and right internal lower chest IR-TRACC x-deflection for target impact speeds of 5, 6, and 7 m/s. While the 6 and 7 m/s tests follow the same loading curve, the test at 5 m/s had a visibly softer loading response, as measured by the left and right lower chest IR-TRACCs. The authors did not observe this behavior in external measurements of penetration and do not have an explanation for the cause.

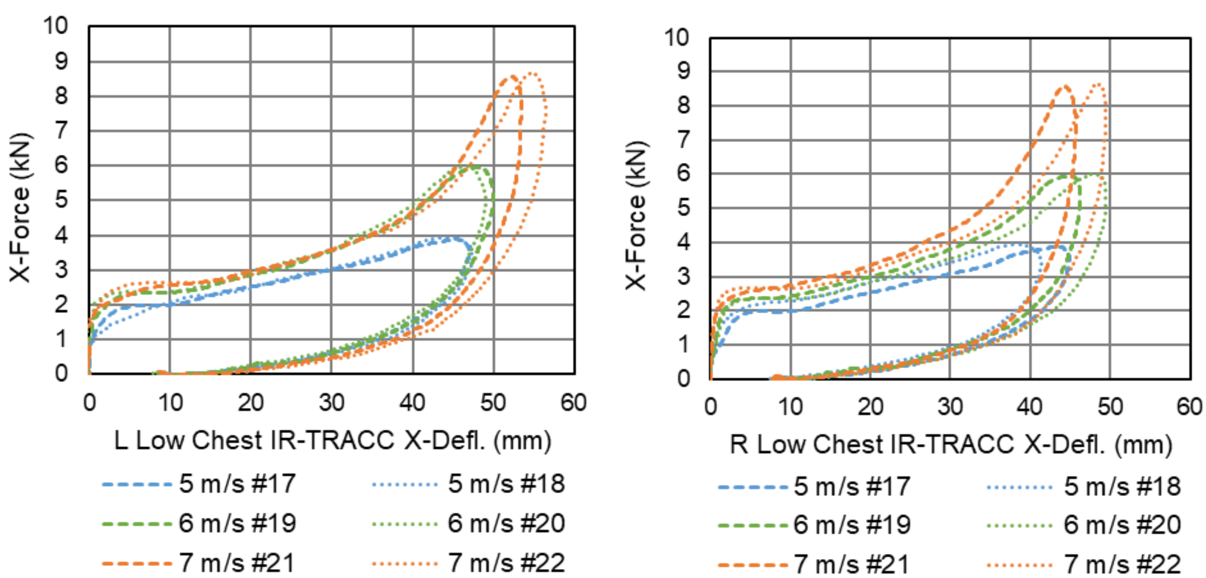


**Figure 17. Lower Chest Velocity Sensitivity Tests – Pendulum X-Force vs L (Left) and R (Right) Lower Chest IR-TRACC X-Deflection with a 24-kg, 50-mm round bar (CFC-180 Forces, CFC-600 Deflections)**

Figure 18 shows peak lower chest VC versus target impact velocity for impacts to the lower chest. Lower chest VC was calculated using x-deflection data from the left and right lower chest IR-TRACCs. A clear relationship between lower chest VC and impact speed was observed.

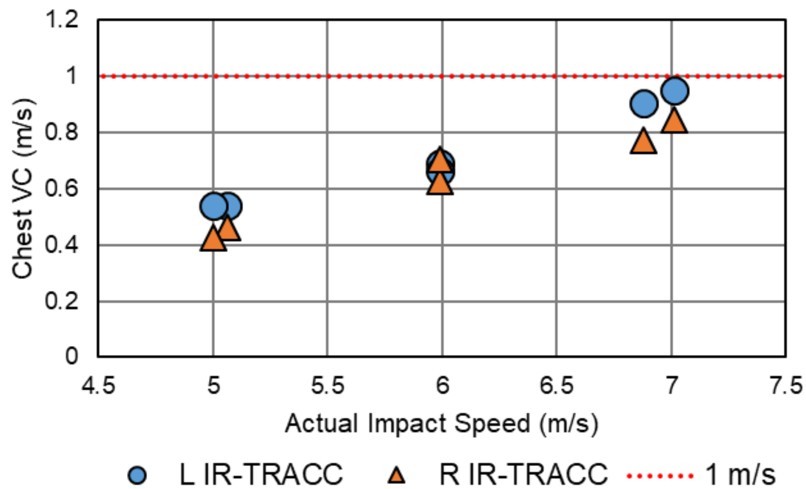


**Figure 18. Lower Chest Velocity Sensitivity Tests – Peak Chest Viscous Criterion versus Measured Impactor Speed (CFC-180 Deflections)**

### *3.3.2 Upper Abdomen Sensitivity Tests*

Figure 19 shows pendulum x-force versus external penetration (estimated using accelerometer data) from impacts to the upper abdomen at target speeds of 3.3, 5.2, and 7 m/s. The force-penetration results from the upper abdomen tests generally followed the same loading curve. Higher peak forces and penetrations were achieved with higher impact speeds.

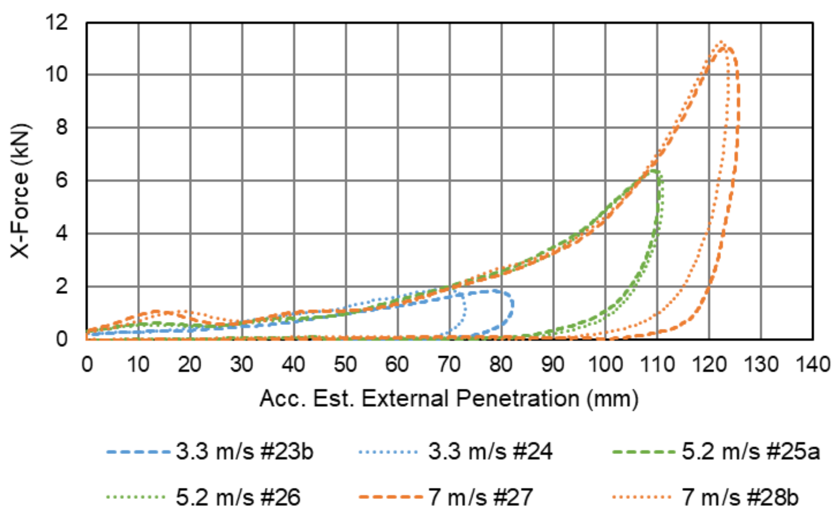


**Figure 19. Upper Abdomen Velocity Sensitivity Tests – Pendulum X-Force vs External Penetration with a 32-kg, 50-mm round bar (CFC-180 Accelerations and Forces)**

Figure 20 shows pendulum x-force versus left and right internal abdomen IR-TRACC x-deflection for each impact speed. While the 5.2 and 7 m/s tests followed the same loading curve, the test at 3.3 m/s had a visibly softer loading response as measured by the left and right abdomen IR-TRACCs. The authors did not observe this behavior in external measurements of penetration and do not have an explanation for the cause. Note that in this test (Test 26) the right abdomen IR-TRACC experienced an instrumentation malfunction, visible at 50 mm of deflection.

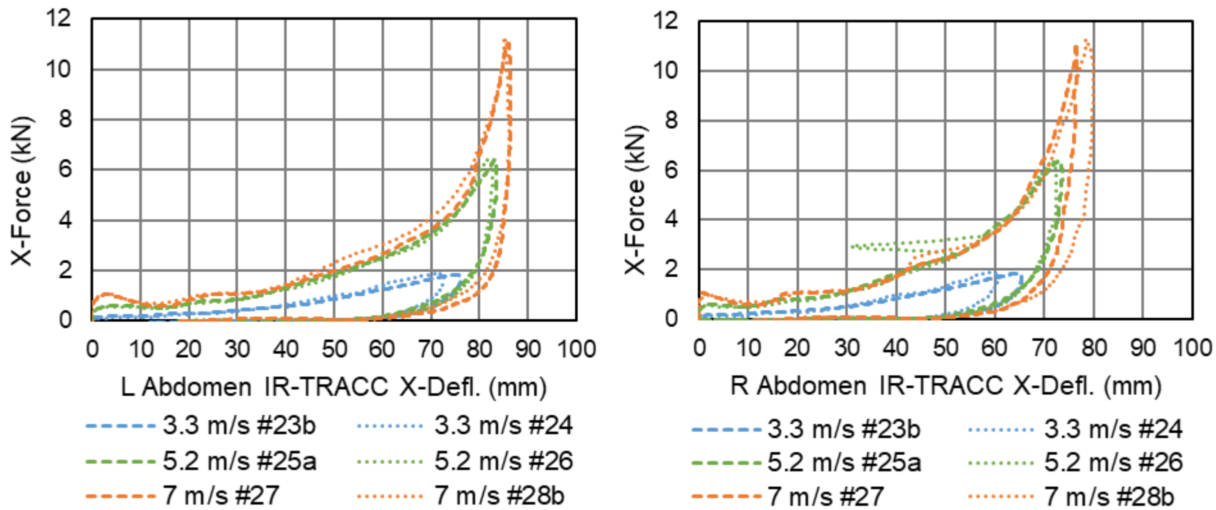


**Figure 20. Upper Abdomen Velocity Sensitivity Tests – Pendulum X-Force vs L (Left) and R (Right) Abdomen IR-TRACC X-Deflection with a 32-kg, 50-mm round bar (CFC-180 Forces, CFC-600 Deflections)**

Figure 21 shows peak abdomen VC versus target impact velocity for impacts to the upper abdomen. Abdomen VC was calculated using x-deflection data from the left and right abdomen IR-TRACCs. A clear relationship between abdomen VC and impact speed was observed.

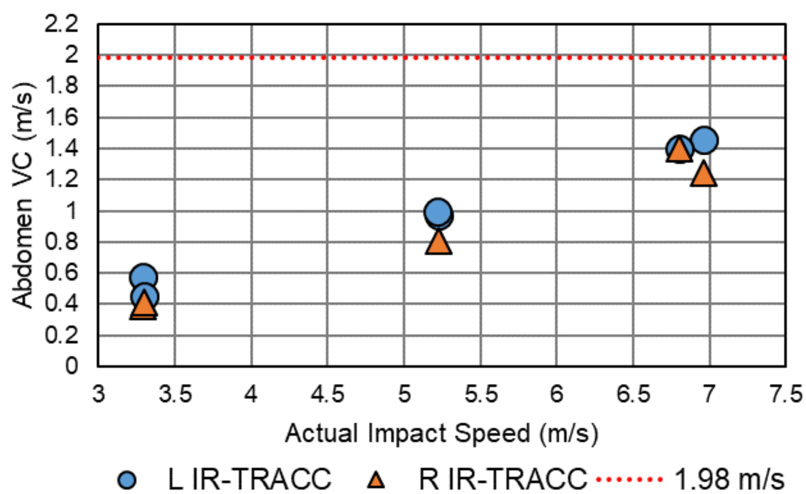


**Figure 21. Upper Abdomen Velocity Sensitivity Tests – Peak Abdomen Viscous Criterion versus Measured Impactor Speed (CFC-180 Deflections)**

Appendix C contains additional results from the velocity sensitivity tests.

# 4. Conclusion

The response of the lower chest and abdomen of the THOR-50M was evaluated in a series of standardized and repeatable pendulum impact tests for frontal impact ATDs. The THOR-50M performed well in the high-energy pendulum impacts and demonstrated good repeatability and durability. However, after Test 1 the right abdomen IR-TRACC suffered an instrumentation malfunction, resulting in fluctuations in the initial tube voltage and making the internal deflection measurements from the right abdomen IR-TRACC unreliable.

The abdomen biofidelity tests (Test 1–3) indicate that the THOR-50M had a similar level of biofidelity as the previous version (THOR-NT) and the H3-RS based on external abdomen deflection measurements. All three ATDs have abdomen bag designs that are based on the original THOR design. Externally, the force-penetration response of the ATDs remained within the biofidelity corridor defined by Cavanaugh [15] up to the same approximate point. Internally, the THOR-50M has a softer force-deflection response due to the difference in instrumentation from the THOR-NT and H3-RS. This internal deflection difference was apparent when evaluating the THOR-50M performance with respect to the THOR-NT lower abdomen certification target.

The performance requirements in APTA PR-CS-S-018 were evaluated using internal measurements from a THOR or H3-RS ATD. The performance requirements were originally proposed [8] when the THOR-NT was widely used. The change in internal abdominal response between the THOR-NT and THOR-50M will be discussed by the APTA PR CS working group in deliberations prior to the next revision of APTA PR-CS-S-018, using these findings to determine whether the abdomen deflection limit should be changed.

For the height sensitivity tests (Tests 4–16a), the highest peak lower chest and abdomen IR-TRACC x-deflections were recorded when the impactor was positioned at the height of the respective sensor. When the impactor was positioned at the height of the lower chest or abdomen IR-TRACCs, the internal versus external compression ratio was approximately 80 percent. When the impactor was not positioned at the height of a sensor, the internal versus external compression ratio was approximately 50 to 60 percent.

The velocity sensitivity tests (Tests 17–28) showed that the THOR-50M was sensitive to changes in impactor velocity. As impact velocity increased, maximum internal and external deflection and VC increased.

In future work, the results from the THOR-50M pendulum impact tests in this study will be compared with those from the H3-RS pendulum impacts to ensure that the option of using either advanced frontal impact ATD is approximately equivalent (from a safety perspective) in APTA PR-CS-S-018. If necessary, FE analysis will be used to compare the ATD performance for pendulum impact conditions (i.e., higher impact velocity and upper abdomen steering wheel biofidelity tests), which were not identical for the pendulum tests described in this report and those by Hynd [9].

## 5. References


[1] Severson, K., and Parent, D. (2006). Train-to-Train Impact Test of Crash-Energy Management Passenger Rail Equipment: Occupant Experiments. ASME, Paper No. IMECE2006-14420.

[2] American Public Transportation Association. (October 2015). Fixed Workstation Table in Passenger Rail Cars (APTA PR-CS-S-018-13, Rev. 1). https://www.apta.com/wp-content/uploads/Standards_Documents/APTA-PR-CS-S-018-13-Rev-1.pdf.

[3] Parent, D., Tyrell, D., Jacobsen K., and K. Severson, K. (2011). Crashworthiness Analysis of the January 26, 2005 Glendale, California Rail Collision. American Society of Mechanical Engineers, Paper No. JRC2011-56132.

[4] Parent, D., Tyrell, D., and Perlman, A.B. (2004). Crashworthiness Analysis of the Placentia, CA Rail Collision. *Proceedings of ICrash 2004, International Crashworthiness Conference*.

[5] Rail Safety and Standards Board. (January 2008). Hybrid III Rail Dummy Specification (T066 Report). https://catalogues.rssb.co.uk/Pages/research-catalogue/PB009352.aspx.

[6] GESAC. (March 2005). THOR Certification Manual. Report No. GESAC-05-04, Revision 2005.2. https://www.nhtsa.gov/sites/nhtsa.dot.gov/files/thorcert05_2.pdf.

[7] Parent, D., Severson, K., and Tyrell, D. (2005). Design of a workstation table with improved crashworthiness performance. American Society of Mechanical Engineers, Paper No. IMECE2005-82779.

[8] Muhlanger, M., Parent, D., Severson, K., and Perlman, B. (2010). Development of Performance Requirements for a Rail Passenger Workstation Table Safety Standard. American Society of Mechanical Engineers, Paper No. RTDF2010-42031.

[9] Hynd, D., and Carroll, J.A. (2017). Abdomen Impact Testing of the Hybrid III Rail Safety (H3-RS) Anthropomorphic Test Device [DOT/FRA/ORD-17/17]. Washington, DC: U.S. Department of Transportation.

[10] Hynd, D., and C. Willis, C. (2017). Sled Tests Using the Hybrid III Rail Safety ATD and Workstation Tables for Passenger Trains [DOT/FRA/ORD-17/10]. Washington, DC: U.S. Department of Transportation.

[11] GESAC. (March 2005). Biomechanical Response Requirements of the THOR NHTSA Advanced Frontal Dummy. Report No. GESAC-05-03, Revision 2005. https://www.nhtsa.gov/sites/nhtsa.dot.gov/files/thorbio05_1.pdf.

[12] National Highway Traffic Safety Administration. (August 2016). THOR 50$^{th}$ Percentile Male (THOR-50M) Qualification Procedures Manual. https://www.nhtsa.gov/sites/nhtsa.dot.gov/files/thor-50m_qualification_august2016.pdf.

[13] SAE. (March 1995). Recommended Practice J211/1 – Instrumentation for Impact Test – Part 1 - Electronic Instrumentation. https://www.sae.org/standards/content/j211/1_199503/ https://www.sae.org/standards/content/j211/1_199503/.

[14] SAE. (February 2015). Recommended Practice J1727 – Calculation Guidelines for Impact Testing. https://www.sae.org/standards/content/j1727_201502/.

[15] Cavanaugh, J.M., Nyquist, G.W., Goldberg, S.J., and King, A.I. (1986). Lower Abdomen Tolerance and Response. *Proceedings of the 30th Stapp Car Crash Conference*.

[16] Nusholtz, G., and Kaiker, P. (1994). Abdominal Response to Steering Wheel Loading. *Proceedings of the 14th International Conference on Experimental Safety Vehicles,* Paper No. 94-S1-O-05.

[17] National Highway Traffic Safety Administration. Biomechanics Test Database. https://www.nhtsa.gov/research-data/databases-and-software.

[18] National Highway Traffic Administration. (December 2001). THOR-Adv: Alpha Users' Manual.

[19] Lau, I., and Viano, D. (1986). The Viscous Criterion – Bases and Applications of an Injury Severity Index for Soft Tissues. SAE Technical Paper No. 861882.

[20] European Union. (May 1996). Directive 96/79 EC of the European Parliament and of the Council on the Protection of Occupants of Motor Vehicles in the Event of a Frontal Impact.

[21] Rail Safety and Standards Board. (December 2010). GM/RT 2100, Issue 4 – Requirements for Rail Vehicle Structures. https://catalogues.rssb.co.uk/rgs/standards/GMRT2100%20Iss%205.pdf.

[22] Viano, D., Lau, I., Asbury, C., King, A., and Begeman, P. (1989). Biomechanics of the Human Chest, Abdomen, and Pelvis in Lateral Impact. *Accident Analysis & Prevention, 21*(6), 553-574.

[23] Viano, D.C., and Lau, V.I. (1988). A Viscous Tolerance Criterion for Soft Tissue Injury Assessment. *Journal of Biomechanics 21* (5), 387-399.

[24] Kent, R., Stacey, S., Kindig, M., Woods, W., Evans, J., and Rouhana, S. (2008). Biomechanical Response of the Pediatric Abdomen, Part 2: Injuries and Their Correlation with Engineering Parameters. SAE Technical Paper No. 2008-22-0006.

[25] Insurance Institute for Highway Safety. (June 1996). Crashworthiness Evaluation Offset Barrier Crash Test Protocol (Version III). https://www.iihs.org/media/43589f5d-b49a-41d5-9eb8-74a2c085321f/8B9rVA/Ratings/Protocols/archive/test_protocol_high_vIII_0696.pdf.

[26] European New Car Assessment Program. (March 2017). Technical Bulletin – Data Format and Injury Criteria Calculation (Version 2.0). https://cdn.euroncap.com/media/27044/tb-021-data-acquisition-and-injury-calculation-v20.pdf.

[27] National Highway Traffic Safety Administration. (August 2018). THOR-50M Procedures for Assembly, Disassembly, and Inspection (PADI). https://www.regulations.gov/document?D=NHTSA-2019-0106-0007.

[28] Haffner, M., Eppinger, R., Rangarajan, N., Shams, T., Artis, M., and Beach, D. (2001). Foundations and Elements of the NHTSA THOR Alpha ATD Design. *17th International Technical Conference on the Enhanced Safety of Vehicles,* Paper No. 458.

## Appendix A.
## Summary of Peak Test Results

Table A1 contains a summary of the left and right peak abdomen IR-TRACC and lower chest IR-TRACC deflections as well as estimates of external penetration by video analysis and accelerometer double integration.

**Table A1. Summary of Peak IR-TRACC X-Deflection Results and Estimates of External Penetration**

| Test | Abdomen IR-TRACC (Defl. CFC-600) | | Lower Chest IR-TRACC (Defl. CFC-600) | | External Penetration (Acc. CFC-180) | |
|---|---|---|---|---|---|---|
| | Left | Right | Left | Right | Video Analysis | Accel. Calc. |
| # | *mm* | *mm* | *mm* | *mm* | *mm* | *mm* |
| 1 | 99.8 | 97.5 | 7.8 | 5.6 | 117.4 | 115.8 |
| 2a | 98.4 | 93.4 | 8.3 | 6.0 | 121.4 | 116.0 |
| 3 | 99.8 | 96.1 | 9.7 | 6.4 | 137.5 | 117.9 |
| 4 | 20.4 | 16.0 | 69.6 | 70.5 | 81.6 | 89.5 |
| 5 | 21.5 | 21.9 | 67.7 | 71.9 | 81.5 | 87.2 |
| 6 | 24.0 | 22.8 | 64.5 | 68.4 | 79.7 | 87.3 |
| 7 | 53.1 | 38.6 | 49.4 | 47.6 | 90.4 | 98.1 |
| 8 | 54.3 | 46.1 | 52.7 | 49.7 | 83.9 | 98.4 |
| 9 | 53.0 | 45.7 | 52.8 | 45.1 | 91.3 | 97.3 |
| 10 | 78.6 | 67.0 | 20.9 | 19.8 | 118.7 | 112.6 |
| 11 | 75.5 | 69.8 | 20.3 | 19.7 | 118.3 | 112.1 |
| 12 | 77.2 | 70.2 | 20.7 | 18.5 | 116.5 | 112.3 |
| 13 | 77.8 | 66.4 | 18.7 | 18.1 | 120.7 | 114.4 |
| 14 | 76.5 | 65.1 | 19.4 | 17.7 | 119.6 | 116.7 |
| 15 | 76.3 | 67.9 | 20.6 | 21.6 | 118.3 | 115.3 |
| 16a | 98.7 | 90.5 | 10.8 | 8.6 | 116.4 | 115.0 |
| 17 | 43.1 | 41.1 | 47.0 | 44.9 | 74.9 | 89.3 |
| 18b | 40.3 | 33.4 | 47.4 | 41.3 | 82.5 | 87.6 |
| 19 | 39.9 | 35.3 | 50.0 | 46.2 | 84.9 | 94.5 |
| 20 | 36.9 | 34.0 | 49.0 | 49.5 | 88.6 | 93.8 |
| 21 | 44.9 | 41.7 | 53.4 | 45.7 | 95.1 | 106.1 |
| 22 | 43.6 | 38.1 | 56.4 | 49.4 | 92.4 | 107.1 |
| 23b | 76.2 | 65.4 | 8.0 | 7.9 | 91.6 | 82.2 |
| 24 | 72.6 | 60.9 | 8.6 | 11.1 | 94.0 | 73.1 |
| 25a | 83.6 | 73.6 | 16.1 | 17.0 | 108.2 | 110.4 |
| 26 | 82.7 | 72.5 | 10.2 | 11.2 | 110.8 | 111.2 |
| 27 | 86.4 | 76.6 | 11.3 | 11.3 | 119.9 | 125.8 |
| 28b | 86.1 | 80.0 | 15.2 | 16.7 | 126.5 | 123.8 |

Table A2 contains a summary of the left and right peak abdomen IR-TRACC and lower chest IR-TRACC viscous criteria.

**Table A2. Summary of Peak IR-TRACC Viscous Criterion Results**

| Test | Abdomen IR-TRACC (Defl. CFC-180) | | Lower Chest IR-TRACC (Defl. CFC-180) | | External Estimates (Acc. CFC-180) | |
|---|---|---|---|---|---|---|
| | **Left** | **Right** | **Left** | **Right** | **Video Analysis** | **Accel. Calc.** |
| | *m/s* | *m/s* | *m/s* | *m/s* | *m/s* | *m/s* |
| 1 | 1.73 | 1.57 | 0.03 | 0.01 | 2.72 | 1.74 |
| 2a | 1.53 | 1.41 | 0.03 | 0.02 | 2.88 | 1.74 |
| 3 | 1.48 | 1.43 | 0.03 | 0.02 | 3.39 | 1.80 |
| 4 | 0.15 | 0.07 | 1.14 | 1.14 | 1.51 | 1.60 |
| 5 | 0.15 | 0.13 | 1.09 | 1.22 | 1.52 | 1.55 |
| 6 | 0.19 | 0.18 | 1.12 | 1.16 | 1.59 | 1.61 |
| 7 | 0.47 | 0.52 | 0.75 | 0.67 | 1.86 | 1.88 |
| 8 | 0.43 | 0.46 | 0.82 | 0.76 | 1.63 | 1.90 |
| 9 | 0.42 | 0.58 | 0.78 | 0.65 | 1.75 | 1.89 |
| 10 | 1.07 | 0.79 | 0.19 | 0.15 | 1.79 | 1.61 |
| 11 | 0.89 | 0.97 | 0.23 | 0.13 | 1.82 | 1.61 |
| 12 | 1.04 | 0.86 | 0.20 | 0.13 | 1.74 | 1.62 |
| 13 | 1.07 | 0.73 | 0.15 | 0.12 | 1.81 | 1.64 |
| 14 | 1.07 | 0.75 | 0.16 | 0.12 | 1.78 | 1.69 |
| 15 | 0.98 | 0.81 | 0.19 | 0.17 | 1.74 | 1.66 |
| 16a | 1.56 | 1.41 | 0.03 | 0.02 | 2.29 | 1.74 |
| 17 | 0.29 | 0.46 | 0.54 | 0.46 | 1.23 | 1.29 |
| 18b | 0.27 | 0.43 | 0.54 | 0.43 | 1.40 | 1.25 |
| 19 | 0.29 | 0.63 | 0.69 | 0.63 | 1.73 | 1.71 |
| 20 | 0.33 | 0.71 | 0.66 | 0.71 | 1.70 | 1.72 |
| 21 | 0.41 | 0.77 | 0.90 | 0.77 | 2.14 | 2.39 |
| 22 | 0.37 | 0.85 | 0.95 | 0.85 | 2.07 | 2.42 |
| 23b | 0.58 | 0.39 | 0.02 | 0.02 | 0.78 | 0.54 |
| 24 | 0.45 | 0.41 | 0.03 | 0.04 | 0.78 | 0.47 |
| 25a | 0.97 | 0.80 | 0.11 | 0.09 | 1.22 | 1.32 |
| 26 | 1.00 | N/A[2] | 0.06 | 0.05 | 1.45 | 1.33 |
| 27 | 1.45 | 1.24 | 0.08 | 0.07 | 1.91 | 2.15 |
| 28b | 1.40 | 1.40 | 0.12 | 0.12 | 1.97 | 2.04 |

[2] Test 26 right abdomen IR-TRACC had an instrumentation malfunction (visible in Figure 13) which made it difficult to calculate VC but not peak deflection.

## Appendix B.
## Height Sensitivity

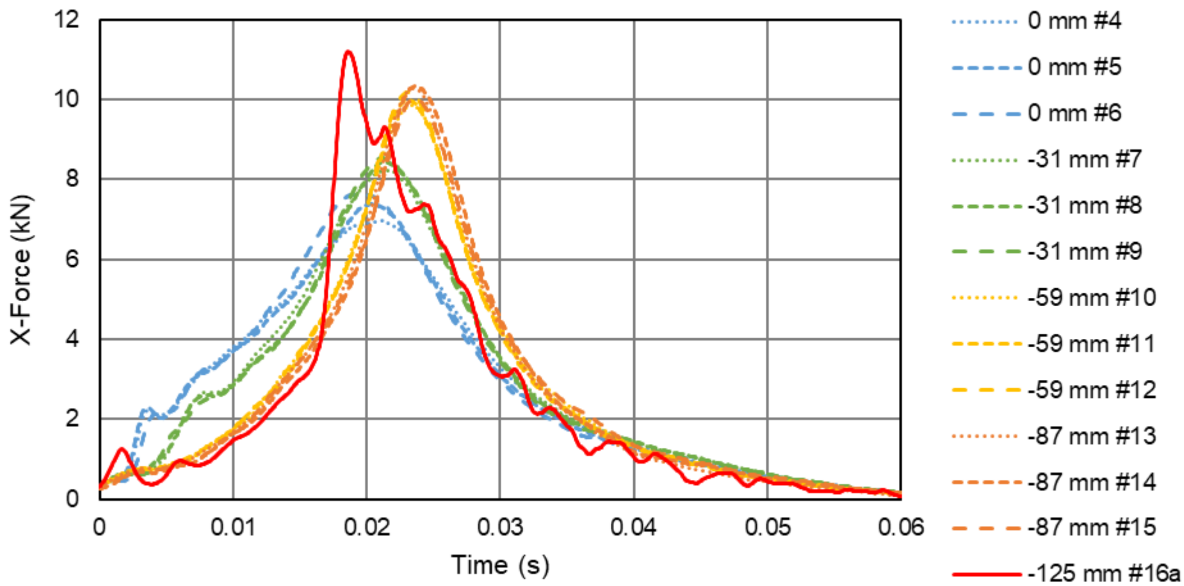


**Figure B1. Impact Height Sensitivity Tests – Pendulum X-Force vs. Time for Impact Heights 0 to 125 mm below 6th Rib (CFC-180 Force)**

### B1. External Results

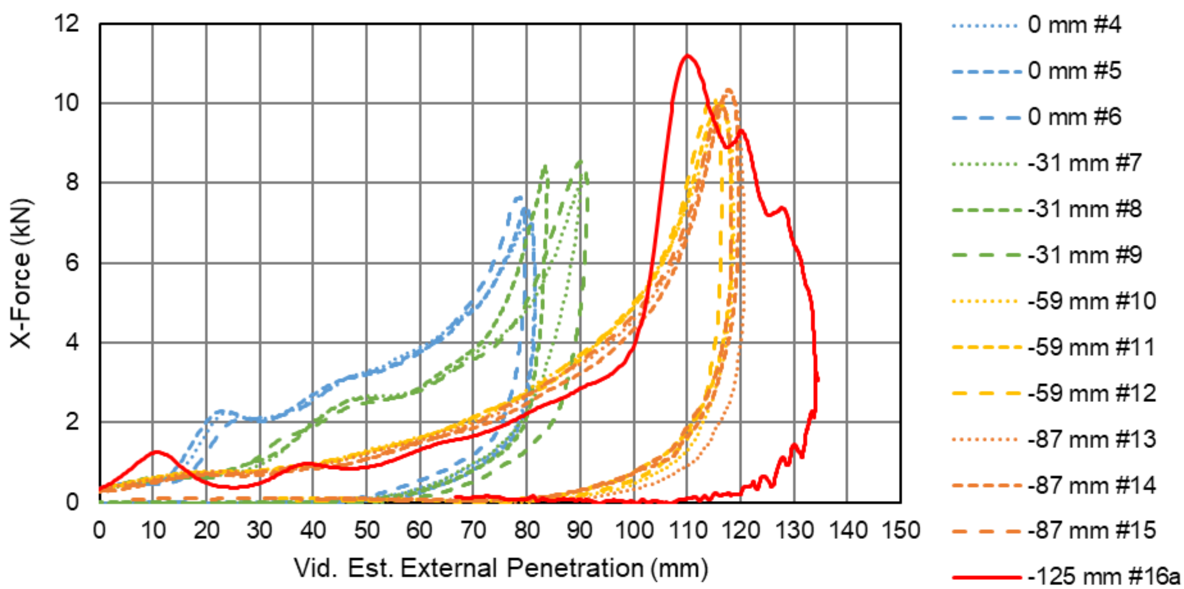


**Figure B2. Impact Height Sensitivity Tests – Pendulum X-Force vs. External Penetration (Video Estimate) for Impact Heights 0 to 125 mm below 6th Rib (CFC-180 Force)**

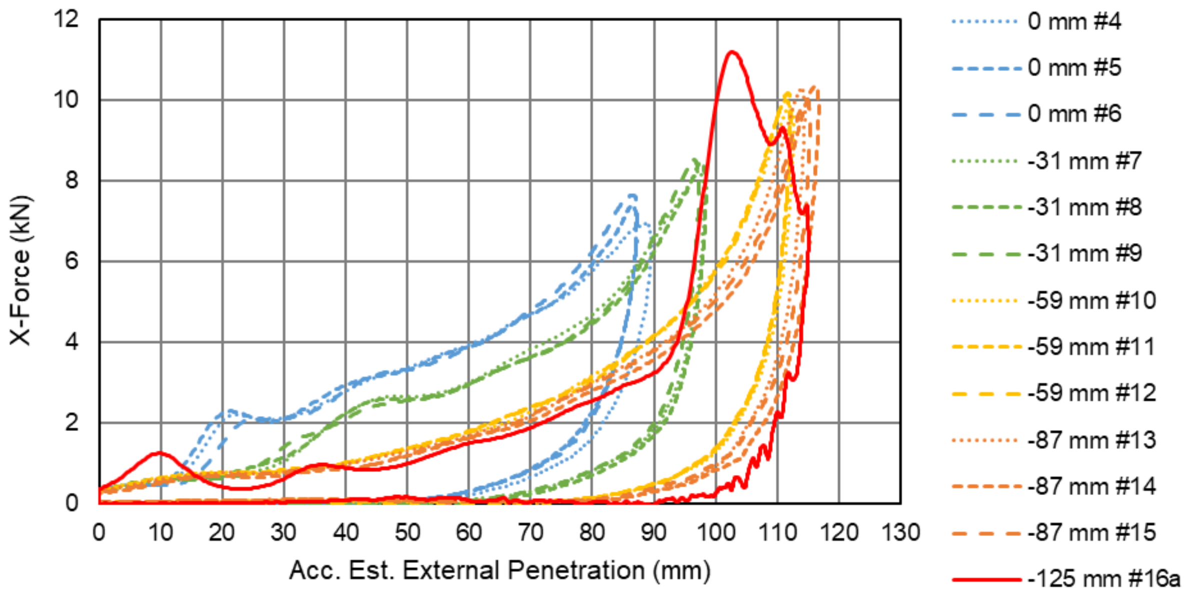


**Figure B3. Impact Height Sensitivity Tests – Pendulum X-Force vs. External Penetration (Accelerometer Estimate) for Impact Heights 0 to 125 mm below 6th Rib (CFC-180 Force and CFC-180 Accelerations)**

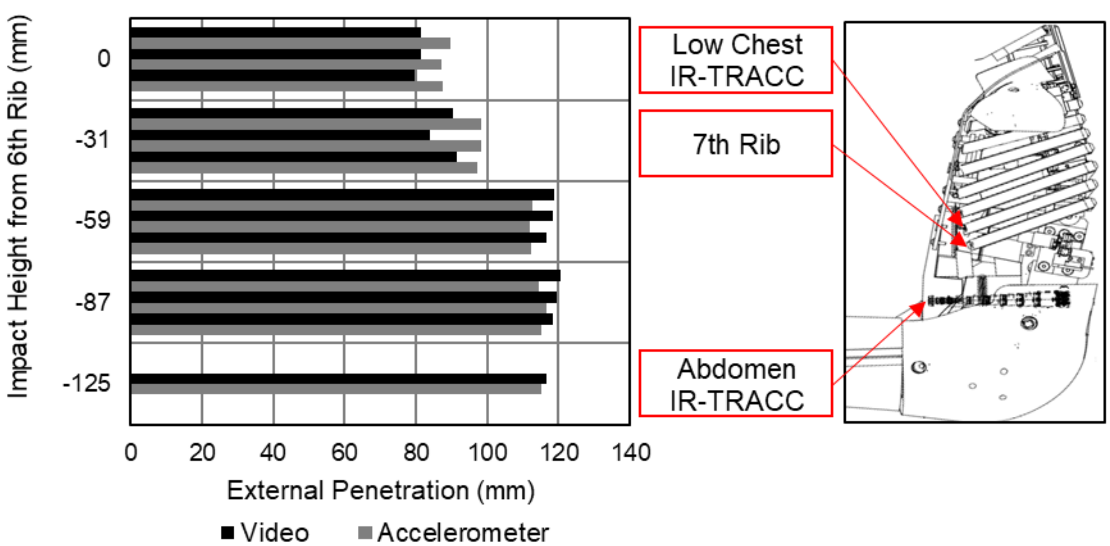


**Figure B4. Impact Height Sensitivity Tests – Peak External Penetration (Video and Accelerometer Estimates) for Impact Heights 0 to 125 mm below 6th Rib (CFC-180 Accelerations)**

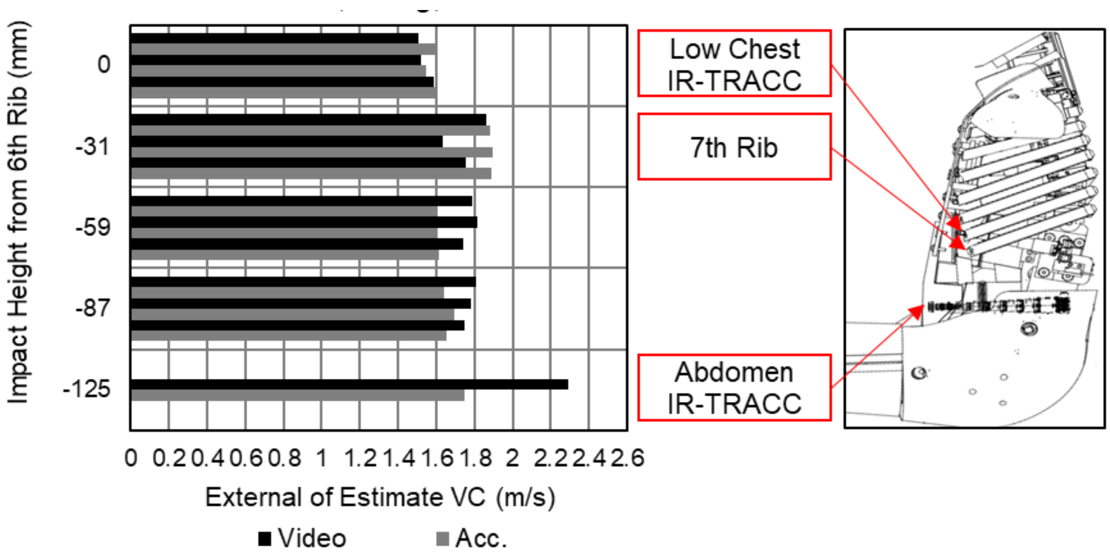


**Figure B5. Impact Height Sensitivity Tests – Peak External Viscous Criterion (Video and Accelerometer Estimates) for Impact Heights 0 to 125 mm below 6th Rib (CFC-180 Accelerations)**

## B2. Lower Chest IR-TRACC Results

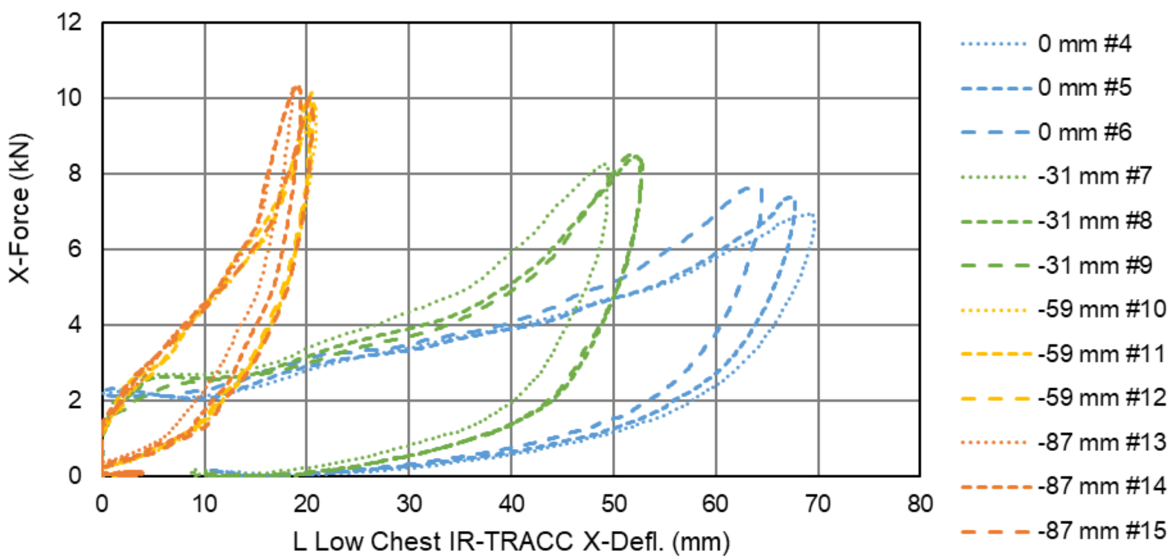


**Figure B6. Impact Height Sensitivity Tests – Pendulum X-Force vs. Left Lower Chest IR-TRACC X-Deflection for Impact Heights 0 to 125 mm below 6th Rib (CFC-180 Force and CFC-600 Deflection)**

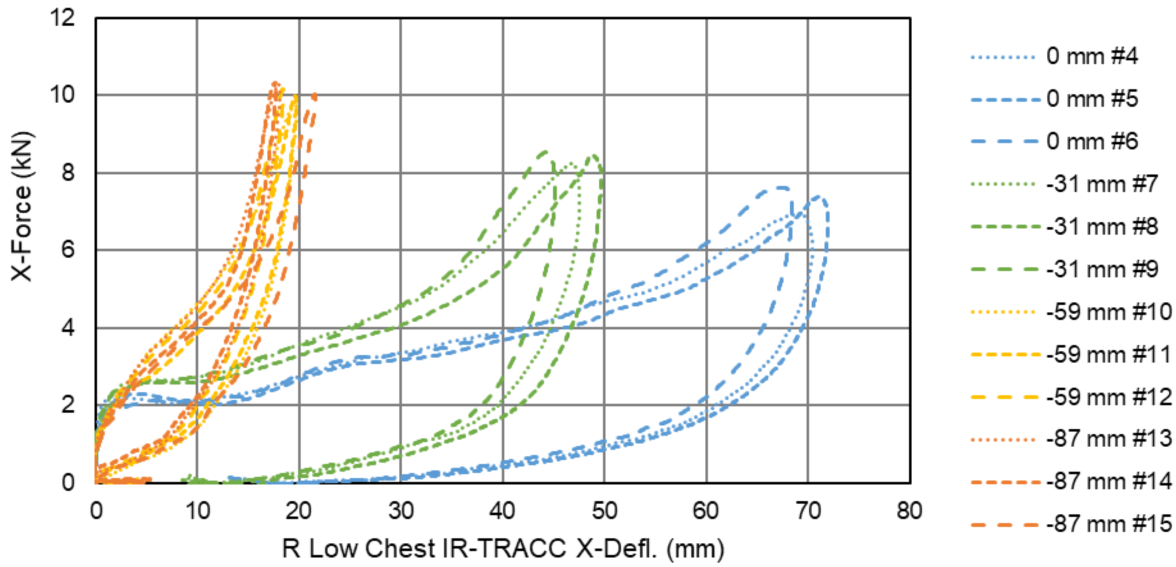


**Figure B7. Impact Height Sensitivity Tests – Pendulum X-Force vs. Right Lower Chest IR-TRACC X-Deflection for Impact Heights 0 to 125 mm below 6th Rib (CFC-180 Force and CFC-600 Deflection)**

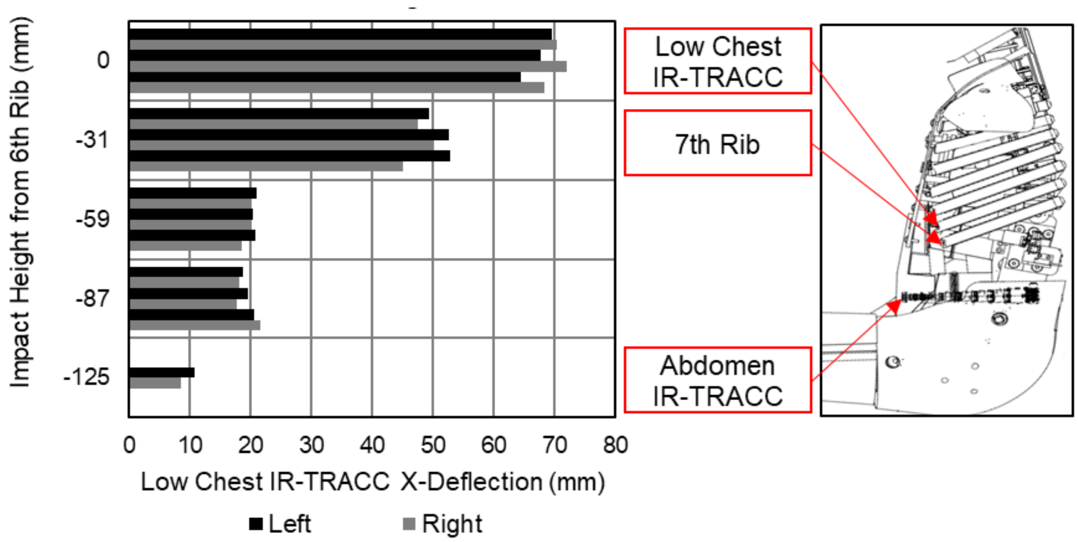


**Figure B8. Impact Height Sensitivity Tests – Peak Lower Chest IR-TRACC X-Deflection for Impact Heights 0 to 125 mm below 6th Rib (CFC-600 Deflections)**

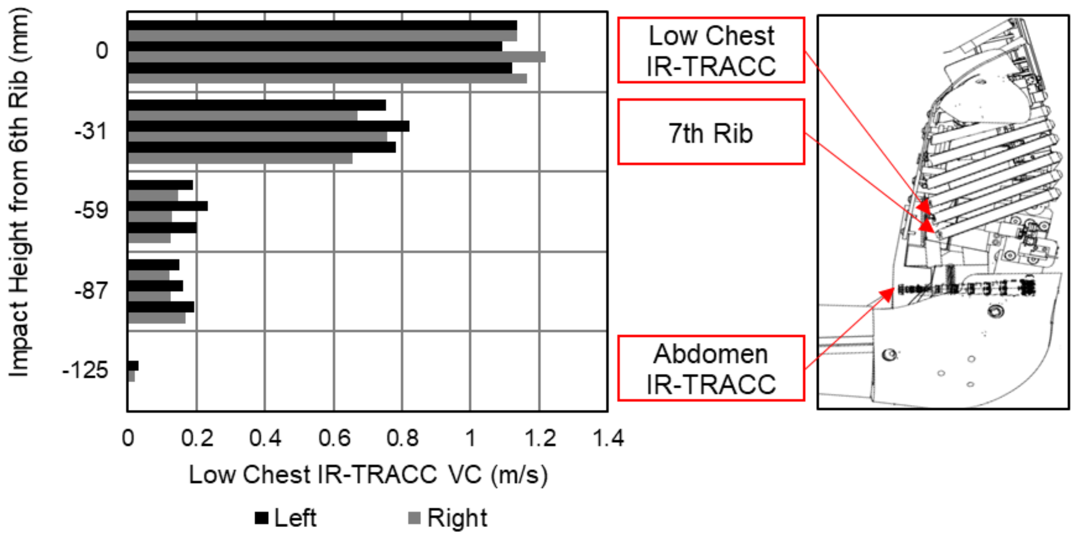


**Figure B9. Impact Height Sensitivity Tests – Peak Lower Chest IR-TRACC Viscous Criterion (VC) for Impact Heights 0 to 125 mm below 6th Rib (CFC-180 Deflections)**

## B3. Abdomen IR-TRACC Results

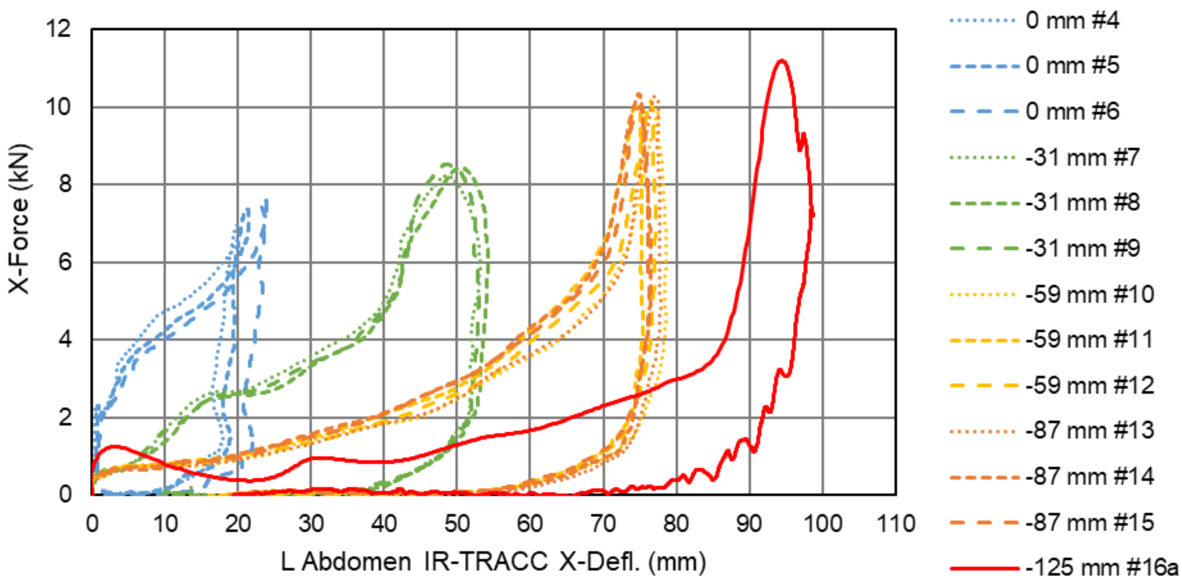


**Figure B10. Impact Height Sensitivity Tests – Pendulum X-Force vs. Left Abdomen IR-TRACC X-Deflection for Impact Heights 0 to 125 mm below 6th Rib (CFC-180 Force and CFC-600 Deflection)**

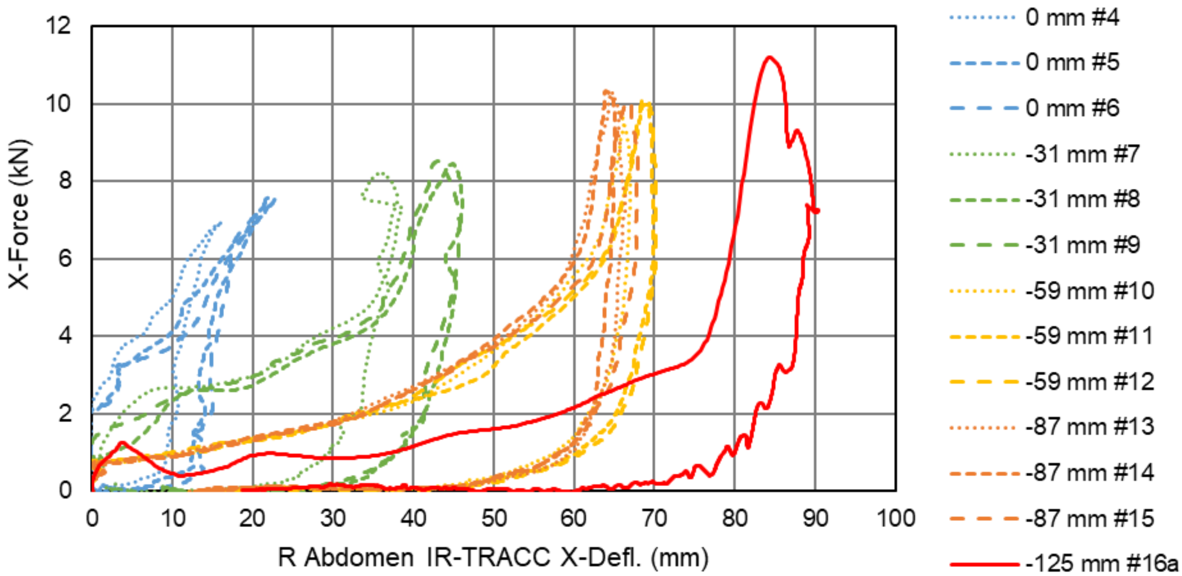


**Figure B11. Impact Height Sensitivity Tests – Pendulum X-Force vs. Right Abdomen X-Deflection for Impact Heights 0 to 125 mm below 6th Rib (CFC-180 Force and CFC-600 Deflection)**

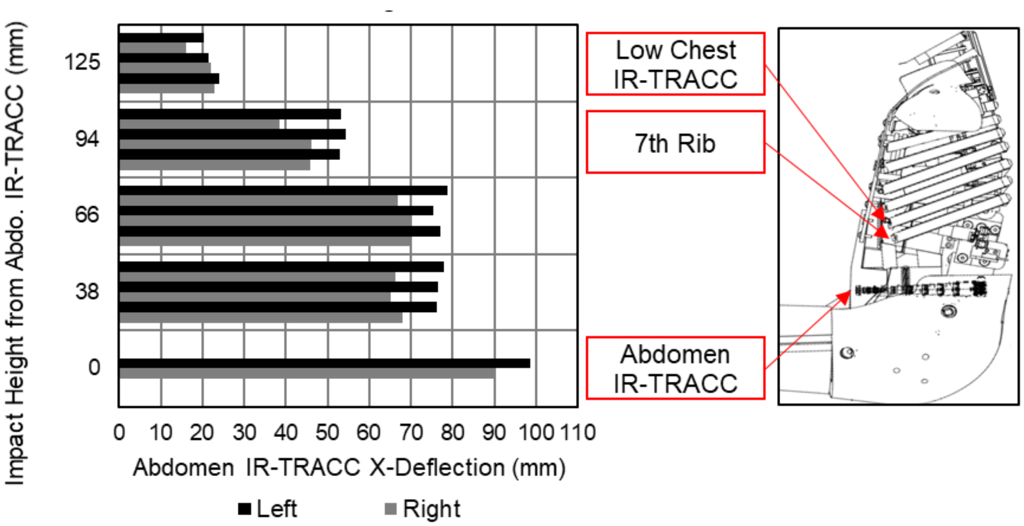


**Figure B12. Impact Height Sensitivity Tests – Peak Abdomen IR-TRACC X-Deflection for Impact Heights 0 to 125 mm below 6th Rib (CFC-600 Deflections)**

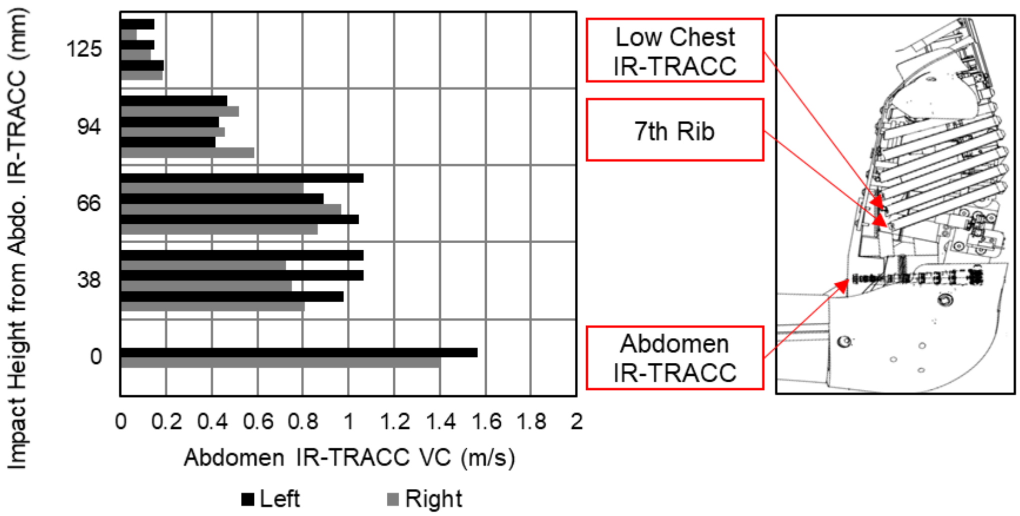


**Figure B13. Impact Height Sensitivity Tests – Peak Abdomen IR-TRACC Viscous Criterion for Impact Heights 0 to 125 mm below 6$^{th}$ Rib (CFC-180 Deflections)**

# Appendix C.
# Velocity Sensitivity

## C1. Chest Velocity Sensitivity

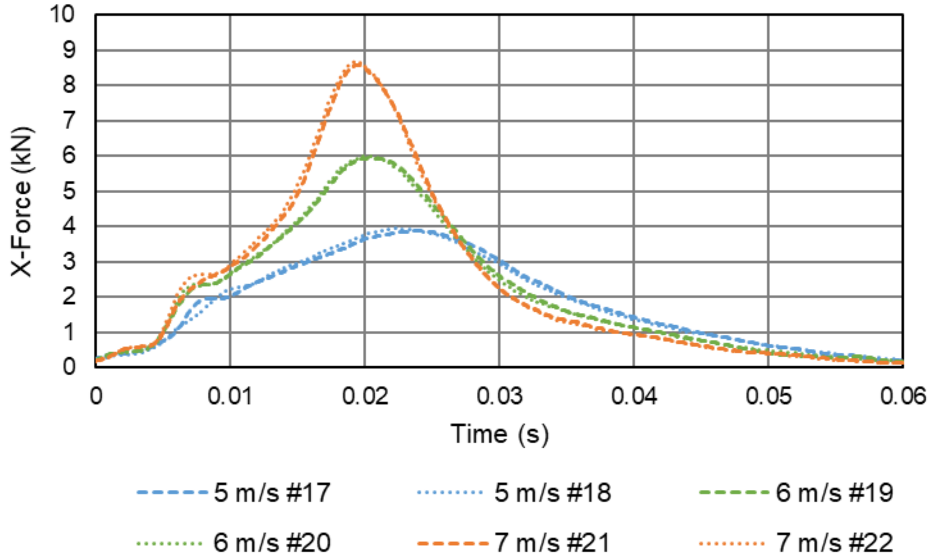


**Figure C1. Lower Chest Velocity Sensitivity Tests – Pendulum X-Force vs. Time for Target Impact Speeds of 5, 6, and 7 m/s (CFC-180 Forces)**

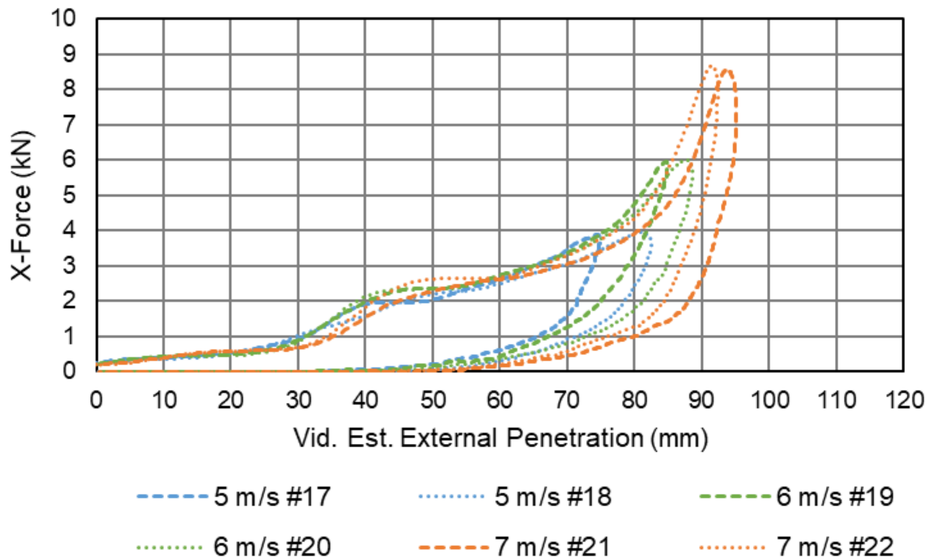


**Figure C2. Lower Chest Velocity Sensitivity Tests – Pendulum X-Force vs. External Penetration (Video Estimate) for Target Impact Speeds of 5, 6, and 7 m/s (CFC-180 Forces)**

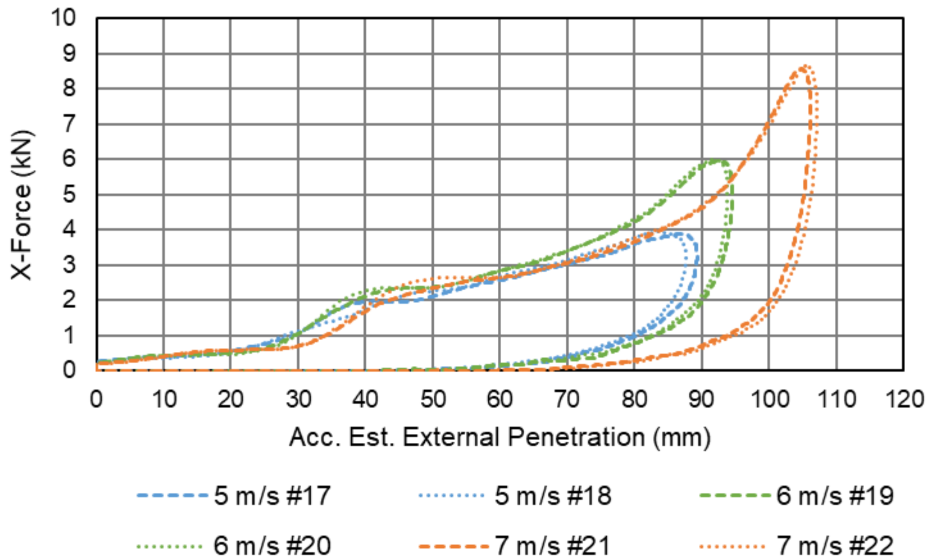


**Figure C3. Lower Chest Velocity Sensitivity Tests – Pendulum X-Force vs. External Penetration (Acceleration Estimate) for Target Impact Speeds of 5, 6, and 7 m/s (CFC-180 Forces and Acceleration)**

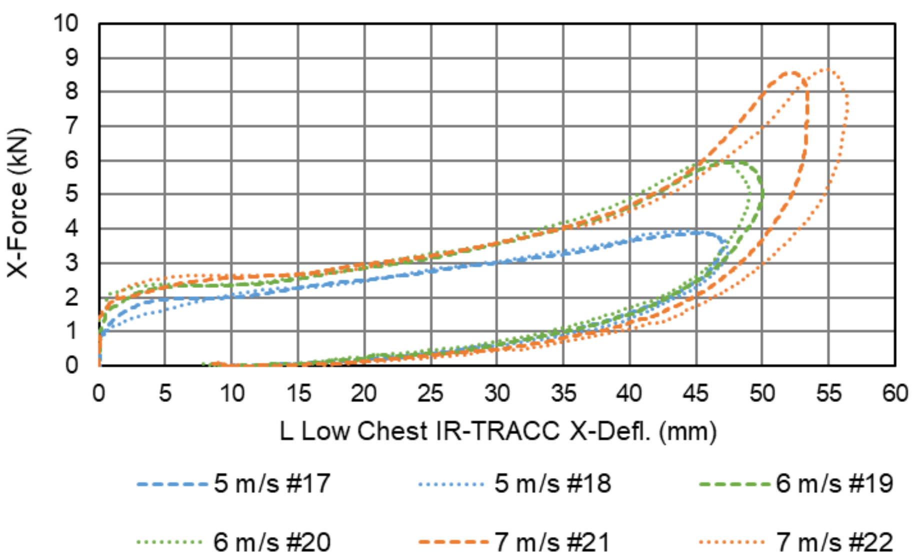


**Figure C4. Lower Chest Velocity Sensitivity Tests – Pendulum X-Force vs. Left Lower Chest IR-TRACC X-Deflection for Target Impact Speeds of 5, 6, and 7 m/s (CFC-180 Forces and CFC-600 Deflections)**

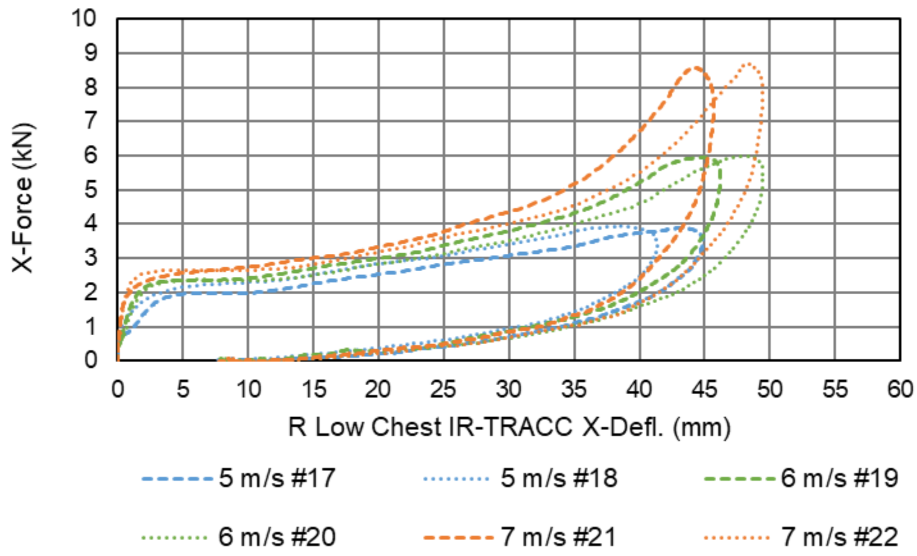


**Figure C5. Lower Chest Velocity Sensitivity Tests – Pendulum X-Force vs. Right Lower Chest IR-TRACC X-Deflection for Target Impact Speeds of 5, 6, and 7 m/s (CFC-180 Forces and CFC-600 Deflections)**

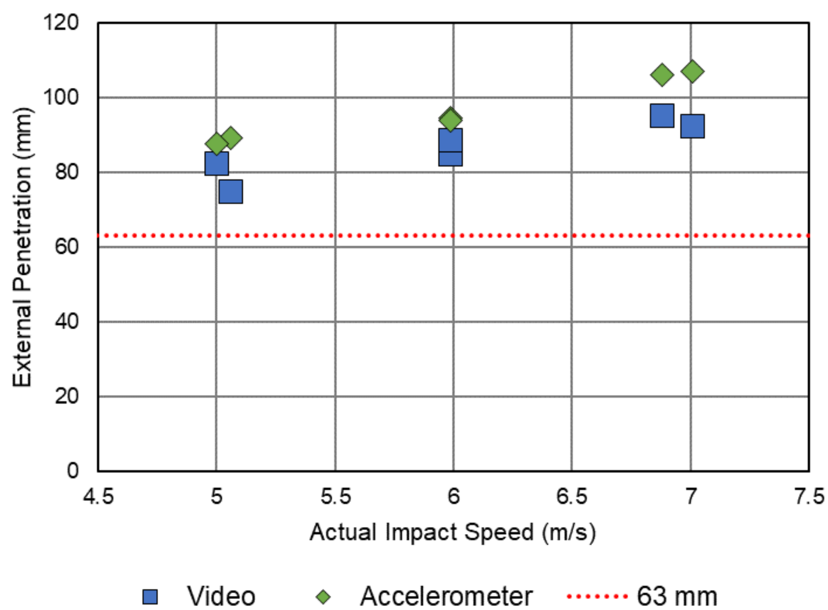


**Figure C6. Lower Chest Velocity Sensitivity Tests – Peak External Penetration vs. Measured Impact Velocity for Target Impact Speeds of 5, 6, and 7 m/s (CFC-180 Accelerations)**

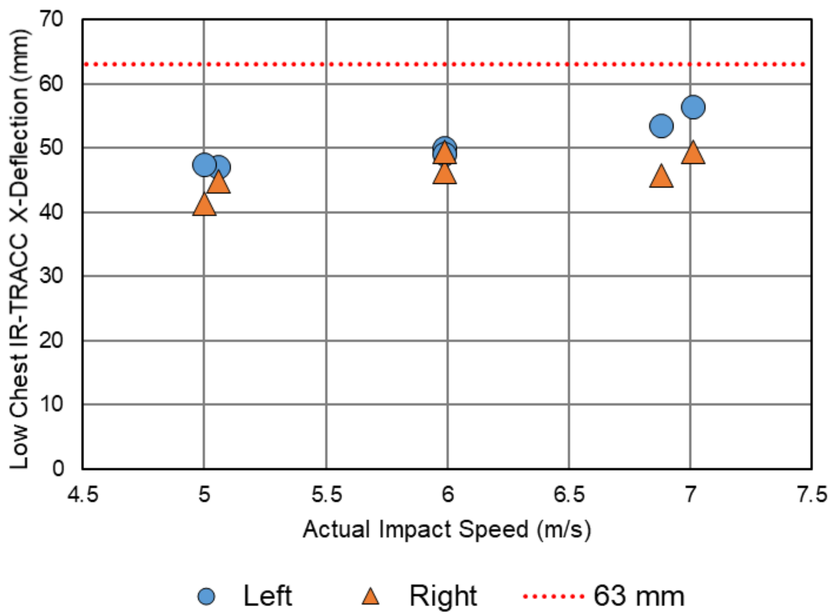


**Figure C7. Lower Chest Velocity Sensitivity Tests – Peak Lower Chest IR-TRACC X-Deflection vs. Measured Impact Velocity for Target Impact Speeds of 5, 6, and 7 m/s (CFC-600 Deflections)**

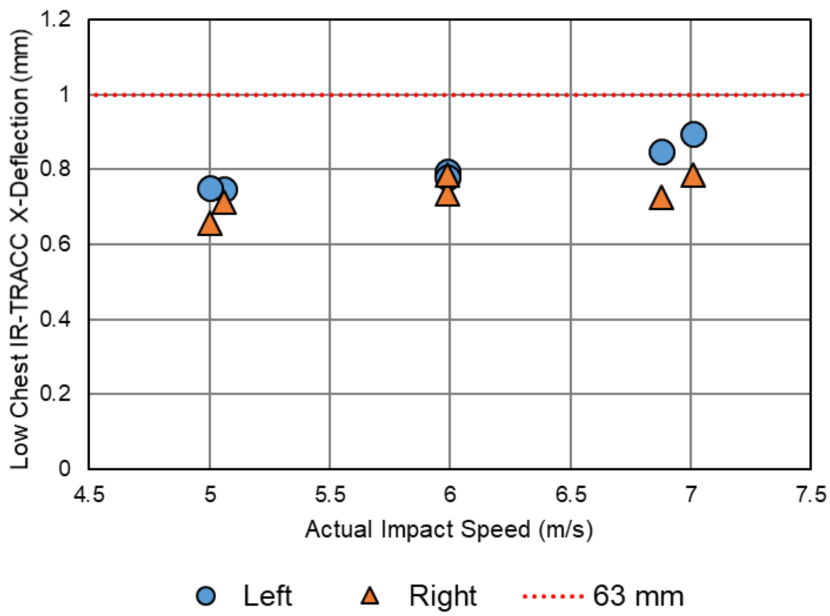


**Figure C8. Lower Chest Velocity Sensitivity Tests – Peak Lower Chest Viscous Criterion vs. Measured Impact Velocity for Target Impact Speeds of 5, 6, and 7 m/s (CFC-180 Deflections)**

## C2. Abdomen Velocity Sensitivity

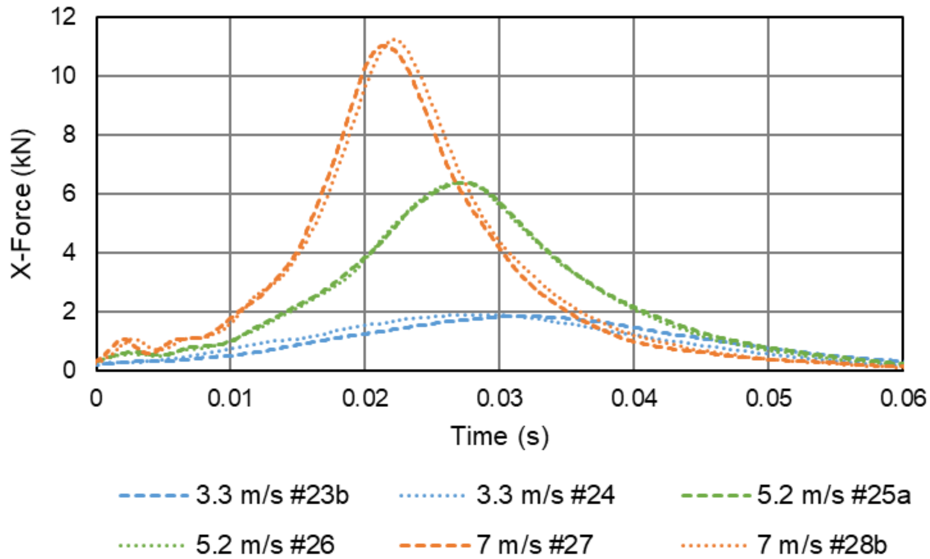


**Figure C9. Upper Abdomen Velocity Sensitivity Tests – Pendulum X-Force vs. Time for Target Impact Speeds of 3.3, 5.2, and 7 m/s (CFC-180 Forces and Accelerations)**

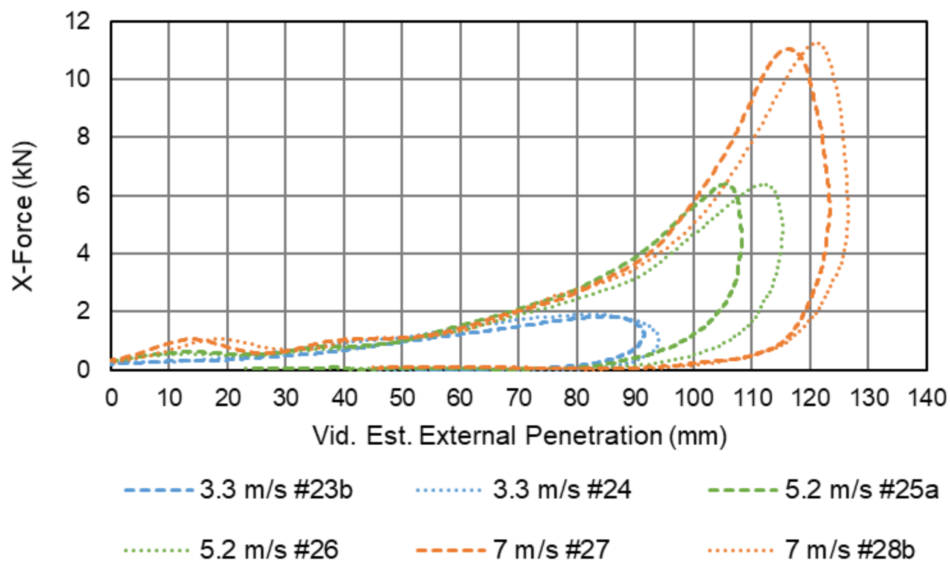


**Figure C10. Upper Abdomen Velocity Sensitivity Tests – Pendulum X-Force vs. External Penetration (Video Estimate) for Target Impact Speeds of 3.3, 5.2, and 7 m/s (CFC-180 Forces and Accelerations)**

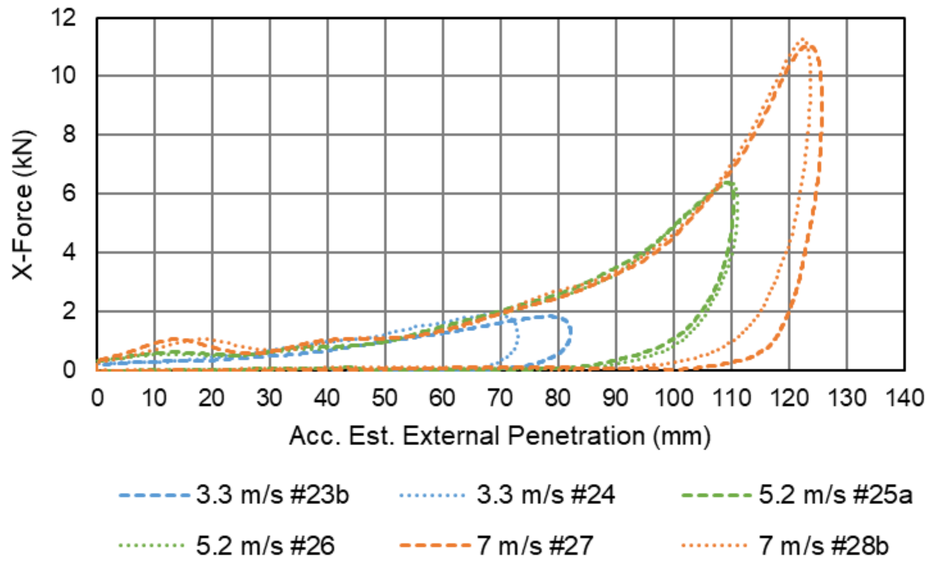


**Figure C11. Upper Abdomen Velocity Sensitivity Tests – Pendulum X-Force vs. External Penetration (Acceleration Estimate) for Target Impact Speeds of 3.3, 5.2, and 7 m/s (CFC-180 Forces and Accelerations)**

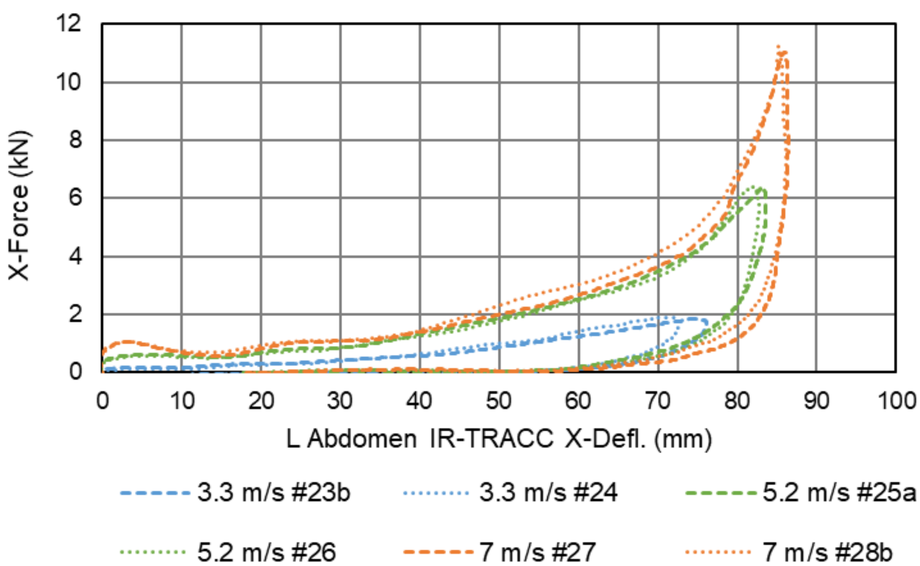


**Figure C12. Upper Abdomen Velocity Sensitivity Tests – Pendulum X-Force vs. Left Abdomen IR-TRACC X-Deflection for Target Impact Speeds of 3.3, 5.2, and 7 m/s (CFC-180 Forces and CFC-600 Deflections)**

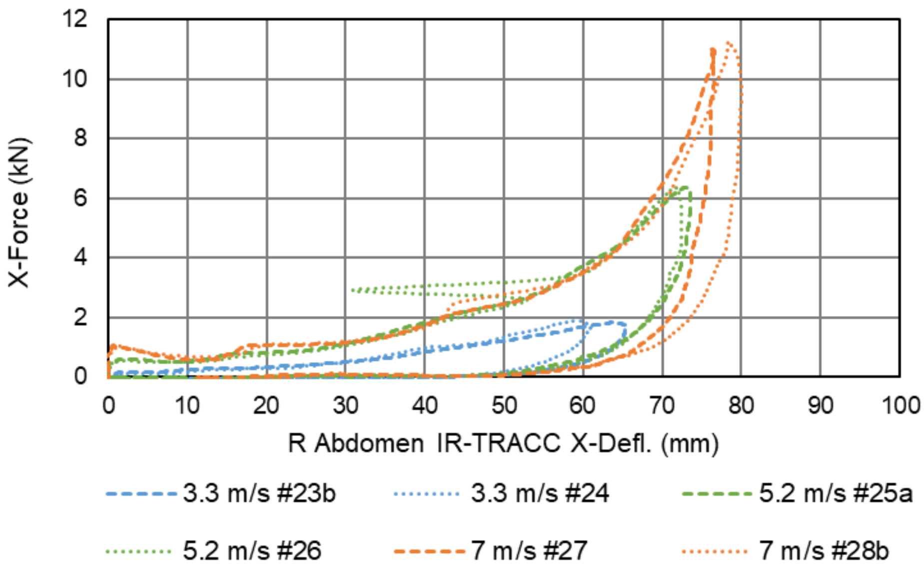


**Figure C13. Upper Abdomen Velocity Sensitivity Tests – Pendulum X-Force vs. Right Abdomen IR-TRACC X-Deflection for Target Impact Speeds of 3.3, 5.2, and 7 m/s (CFC-180 Forces and CFC-600 Deflections)**

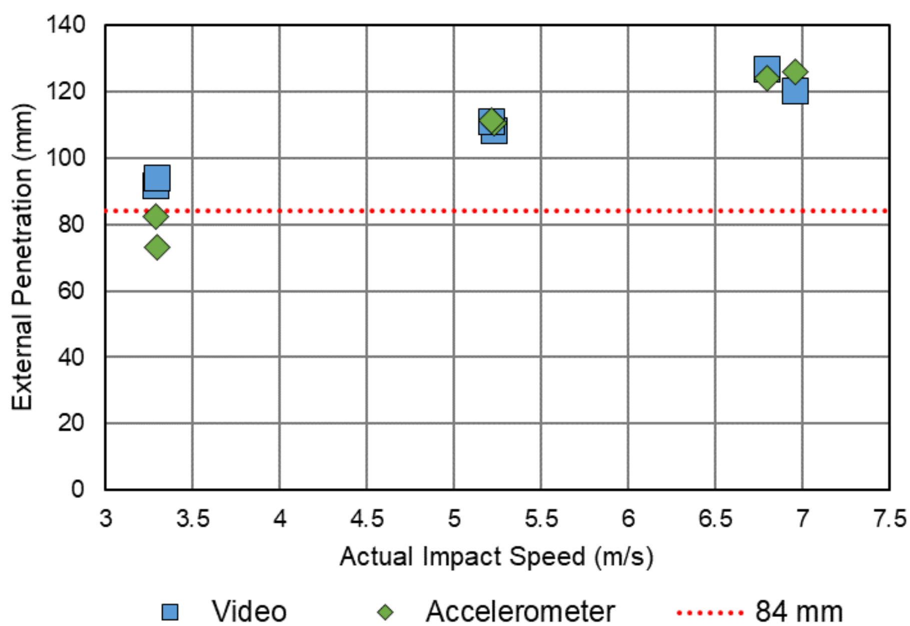


**Figure C14. Upper Abdomen Velocity Sensitivity Tests – Peak External Penetration vs. Measured Impact Velocity for Target Impact Speeds of 3.3, 5.2, and 7 m/s (CFC-180 Accelerations)**

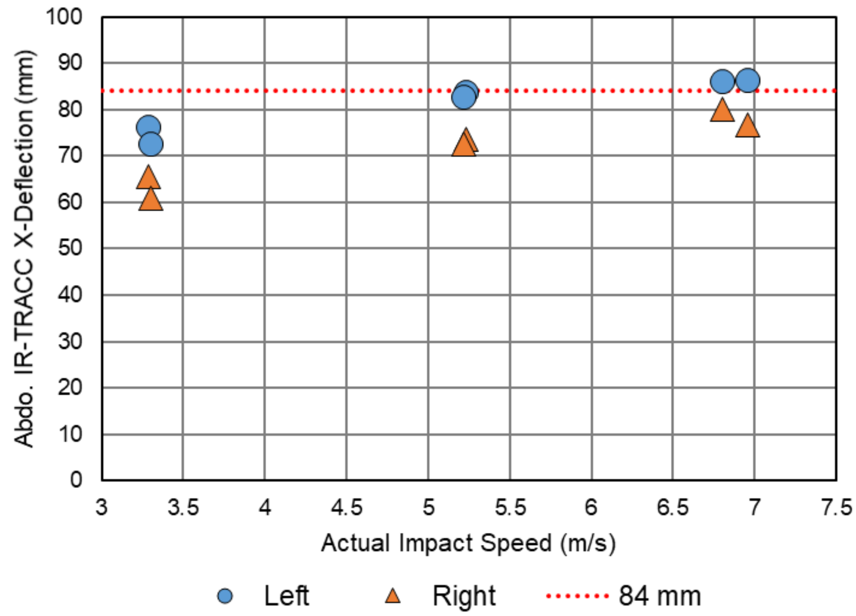


**Figure C15. Upper Abdomen Velocity Sensitivity Tests – Peak Abdomen IR-TRACC X-Deflection vs. Measured Impact Velocity for Target Impact Speeds of 3.3, 5.2, and 7 m/s (CFC-600 Deflections)**

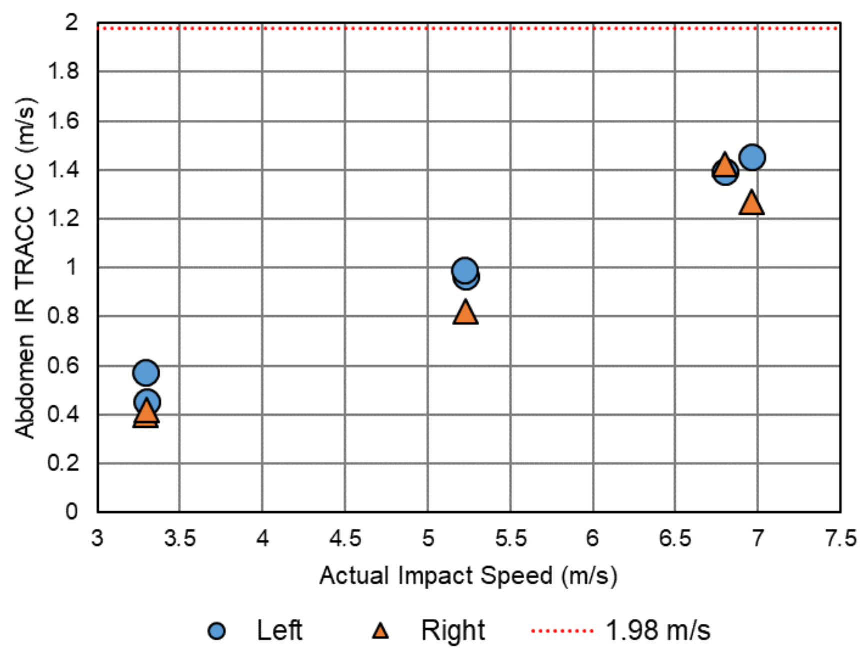


**Figure C16. Upper Abdomen Velocity Sensitivity Tests – Peak Abdomen Viscous Criterion vs. Measured Impact Velocity for Target Impact Speeds of 3.3, 5.2, and 7 m/s (CFC-180 Deflections)**

# Appendix D. Viscous Criterion

The chest viscous criterion (VC) is an injury criterion proposed by Lau and Viano for blunt force trauma to the chest [19]. Lau and Viano intended chest VC to describe rate-dependent modes of soft tissue injury as a supplement to the already-established chest compressive deflection injury criterion.

Chest VC is calculated per Equation D1 where:

- $D_C$ is the undeformed depth of the chest
    - $D_C$ is defined as 229 mm for the H3-50M, H3-RS, and THOR-50M
- $D(t)$ is the CFC filtered instantaneous compressive chest deflection measured by
    - a sternum rotary potentiometer in the H3-50M
    - negative x-axis displacement of four CRUX sensors in H3-RS
    - negative x-axis displacement of four IR-TRACC sensors in the THOR-50M
- $C(t)$ is the instantaneous chest compression ratio
    - $C(t)$ is defined as $D(t)$ divided by $D_C$
- $\alpha$ is the proportionality factor used to scale internal chest VC to external chest VC
    - $\alpha$ is defined as 1.3 for the H3-50M, H3-RS, and THOR-50M
- $V(t)$ is the chest compression velocity calculated as the first derivative of $D(t)$ using a five-point stencil for numerical differentiation
- $\Delta t$ is the time step (interval) and must be less than or equal to $1.25 \times 10^{-4}$ seconds.

**Equation D1. Calculation of Chest Viscous Criterion (VC)**

$$Chest\ VC = |\alpha \cdot V(t) \cdot C(t)|$$

$$C(t) = \frac{D(t)}{D_c}$$

$$V(t) = \frac{8[D(t+\Delta t) - D(t-\Delta t)] - [D(t+2\Delta t) - D(t-2\Delta t)]}{12\Delta t}$$

A constant $(\alpha)$ of 1.3 is used to scale internal measurements of chest VC to an estimation of the external chest VC. This scaling factor is referred to as a proportionality factor by Lau and Viano. It was determined by comparing maximum external and internal measurements of $C(t)$ and $V(t)$ on a H3-50M impacted with a 23.4-kg, 6.7-m/s pendulum.

Lau and Viano concluded from human cadaver studies that a chest VC of 1.0 m/s corresponds to 25 percent probability of a severe thoracic injury (AIS 4+) while a chest VC of 1.2 m/s corresponds to a 25 percent probability of a fatal thoracic injury (AIS 5+). The injury assessment reference value (IARV) of 1.0 m/s corresponding to 25 percent risk of AIS 4+ injury was eventually chosen as a suitable performance limit.

In 1996, the European Union (EU) issued Directive 96/79 for Frontal Crash Protection [20], setting a performance limit of 1.0 m/s for chest VC in a 56-km/h frontal crash scenario; however, the analogous frontal crash safety regulation in the U.S. (49 CFR 571.208) does not have a requirement on chest VC.

In 2010, the chest VC performance limit was also adopted in GM/RT 2100, Issue 4 – Requirements for Rail Vehicle Structures [21] by the Rail Safety Standards Board (RSSB) in the U.K. for a workstation table sled test with a minimum 5g crash pulse. In 2013, the APTA Workstation Table Safety Standard (APTA-PR-CS-S-018-13) also set a chest VC performance limit of 1.0 m/s with a minimum 8g crash pulse.

While motor vehicle frontal crash scenarios do not have a widely agreed-upon abdominal viscous criterion, GM/RT 2100 proposed an abdominal VC performance limit of 1.98 m/s. A proportionality factor of 1 is used for abdominal VC and the depth of the uncompressed abdomen test device is not specified in GM/RT 2100. Since APTA S-018 was first published, the abdomen VC performance limit was set at 1.98 m/s, and the undeformed abdomen depth was not specified. Volpe has proposed to add the measured undeformed depth of the H3-RS abdomen (245 mm) and the THOR-50M abdomen (252 mm) to Revision 2 of APTA S-018 to standardize the calculation procedure.

While GM/RT 2100 does not explicitly state the source of the abdomen VC performance limit, the injury assessment reference value (IARV) from Viano et al. [22] appears to be the basis for the performance limit in GM/RT 2100. Muhlanger et al. [8] commented that the abdominal VC IARV proposed by Viano was determined from side impact tests which may not be appropriate for frontal impacts. The IARV corresponds to a 25 percent risk of an AIS 4+ injury from a side impact. Other work by Viano and Lau [19] [23] suggest that a VC of 1.98 m/s would correspond to a much higher risk of an AIS 4+ injury for an upper abdomen injury due to steering wheel loading. Additionally, work by Kent et al. [24] also indicate that that a VC of 1.98 m/s would correspond to a high risk of an AIS 3+ injury for a lower abdomen injury from seat belt loading.

There is not unanimous consensus in the literature on the usefulness of VC as a predictor of risk of injury. Kent argues that the supposed rate-dependent link between injury and VC is principally due to the well-established link between the compression ratio and injury and not a link between compressive deflection rate and injury [24].

## D1. Filtering

APTA S-018 and GM/RT 2100 require that chest and abdomen deflections be filtered with a channel frequency class (CFC) 600 filter per SAE J211/1 [13]. This filtering procedure is also recommended by the Insurance Institute for Highway Safety (IIHS) [25].

In contrast to this, EU Directive 96/79 and European New Car Assessment Program (EuroNCAP) [26] require filtering of deflections at CFC 180. This difference in cutoff frequency would not typically affect a pass/fail outcome for peak compressive chest or abdomen deflection because the chest and abdomen deflection time history signals are predominantly low frequency. However, VC is calculated as a derivative and is much more sensitive to low-pass filtering. Because of this sensitivity to high frequency noise, SAE J1727 [14] was recently updated in 2010 to recommend lowering the CFC class from 600 to 180.

Figure D1 shows the unfiltered (raw) x-deflection time histories from the left and right abdomen IR-TRACCs from Test 1.

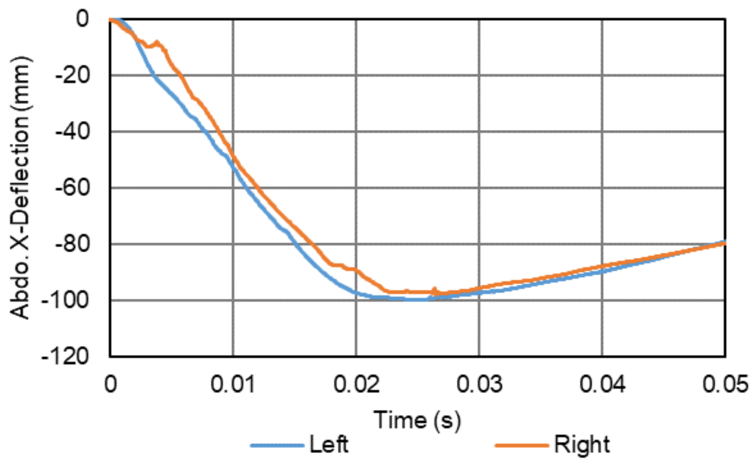


**Figure D1. Abdomen IR-TRACC X-Deflection vs. Time in Test 1 (Unfiltered Deflections)**

Figure D2 shows the first derivative (x-velocity) of the abdomen IR-TRACC x-deflections shown in Figure D1 after the x-deflections were filtered at CFC-600 and CFC-180 per the THOR-50M Procedures for Assembly, Disassembly, and Inspection (PADI) [27]. While there was not a noticeable change in peak x-deflection after filtering (not shown), there is a noticeable change in x-velocity.

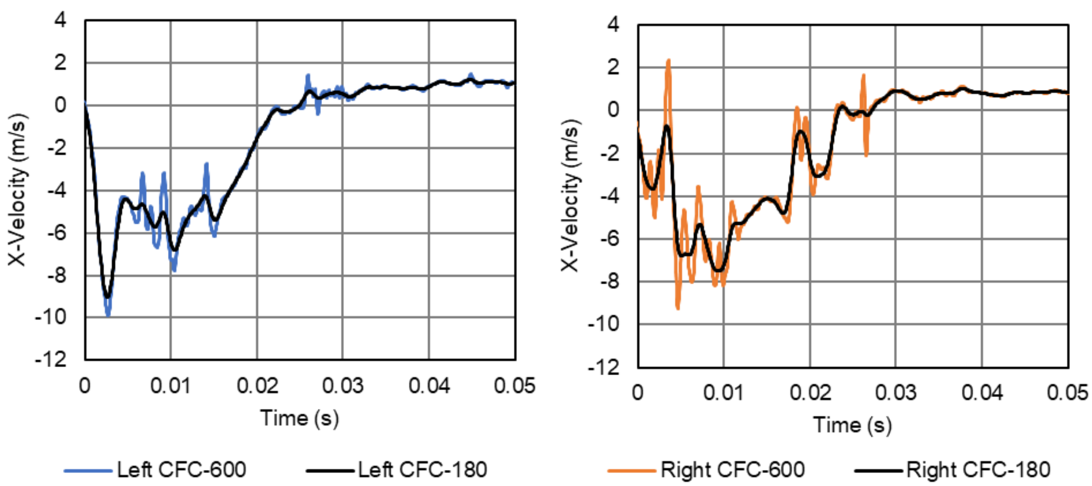


**Figure D2. Abdomen IR-TRACC X-Velocity (First Derivative of X-Deflection) vs. Time in Test 1 with CFC-600 and CFC-180 Filtered X-Deflections**

Figure D3 shows VC from the abdomen IR-TRACCs, calculated per Equation D1, which shows a dependence on choice of CFC filter resulting from the x-velocity dependence described above. It is clear here that the choice of filter could easily affect a pass/fail outcome from a dynamic table test (abdomen VC < 1.98 m/s).

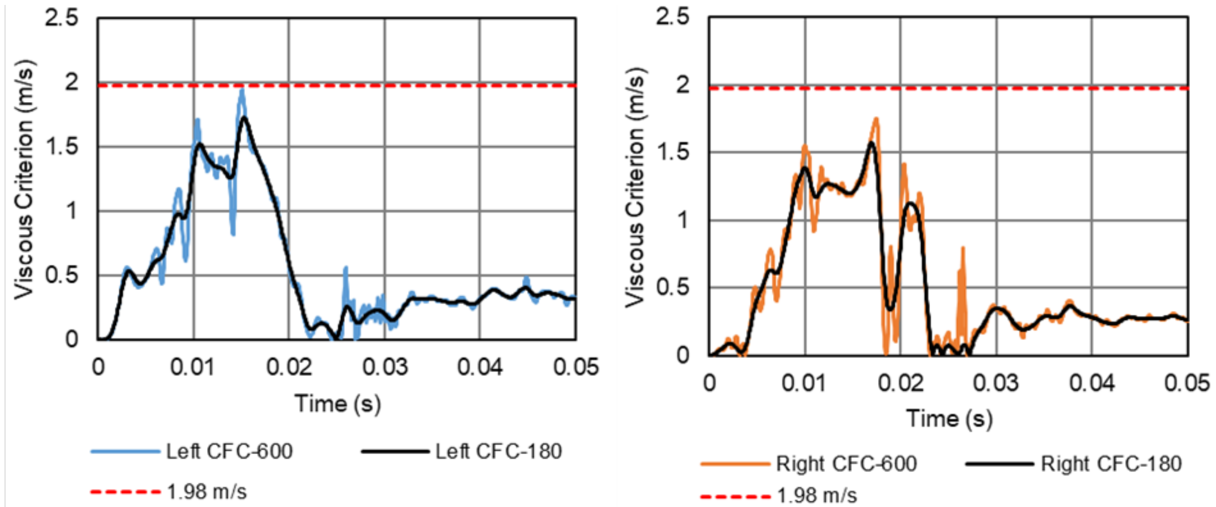


**Figure D3. Abdomen IR-TRACC Viscous Criterion (VC) vs. Time in Test 1 with CFC-600 and CFC-180 Filtered X-Deflections**

The results from this study on filtering VC will be used to inform technical discussions on the choice of CFC filter within the APTA PR CS working group while revising APTA-PR-CS-S-018-13. Currently, Revision 1 of the standard references SAE-J211 and specifies a CFC-600 filter for chest deflection, and no explicit procedures are stated for chest VC in SAE-J211. The authors propose that Revision 2 of the standard should reference SAE-J1727 and specify a CFC-180 filter for VC due to high-frequency noise having a significant effect on the calculation of rate of compression (velocity).

# Appendix E. Proportionality Factor

In their work on VC, Lau and Viano also proposed a proportionality (scaling) factor to transform internal measurements from a H3-50M ATD to estimates of external measurements [19]. In the calculation of chest VC (Equation D1), the proportionality factor is termed $\alpha$. In Lau and Viano's study, a seated H3-50M was impacted twice with a 23.4-kg pendulum at a velocity of 6.7 m/s, using an impactor shaped like a steering column. External deformation was measured by high-speed video analysis, and internal deformation was measured by the H3-50M chest (sternum) rotary potentiometer. For maximum deformation, 82 mm was recorded externally and 68 mm was recorded internally. For maximum deformation velocity (first derivative), 6.1 m/s was recorded externally and 5.8 m/s was recorded internally. A simple linear relationship was derived for maximum external versus internal deformation and deformation velocity, as shown in Equation E1.

**Equation E1. Calculation of Chest Viscous Criterion Proportionality Factor by Lau and Viano [19]**

$$\alpha_{def} = \frac{82\,mm}{68\,mm} \approx 1.2$$

$$\alpha_{vel} = \frac{6.1\,m/s}{5.8\,m/s} \approx 1.1$$

$$\alpha = \alpha_{def} \cdot \alpha_{vel} \approx 1.3$$

Lau and Viano's estimation of a proportionality factor for chest VC of a H3-50M is a straightforward calculation. The same methodology was applied to the THOR-50M for impacts centered at the height of the lower chest IR-TRACCs and abdomen IR-TRACCs. Impacts which were not centered on a set of IR-TRACCs were excluded as the internal measurements were sensitive to height as discussed in Section 3.2. The tests which were used for calculation of proportionality factor were the height sensitivity tests (32-kg, 6.1-m/s, 2-inch round bar) centered on the $6^{th}$ rib IR-TRACCs (Tests 4, 5, 6) and abdomen IR-TRACCs (Test 16a) and the lower abdomen biofidelity tests (Tests 1, 2a, 3). In all cases the accelerometer estimation of external VC was used because of difficulty determining time zero in the high-speed video estimation, as discussed in Section 2.2. For internal (IR-TRACC) VC, the maximum VC measured from the left and right IR-TRACCs was used to calculate proportionality factor.

Table E1 shows the maximum internal (IR-TRACC) and external lower chest VC and proportionality factors. The average of the proportionality factors was 1.35, with a standard deviation of 0.07. Table E2 shows the maximum internal (IR-TRACC) and external abdomen VC and proportionality factors. The average of the proportionality factors was 1.12, with a standard deviation of 0.09. Note that the only abdomen IR-TRACC impact which did not show signs of interaction between the impactor and ASIS parts (refer to Section 2.3.2) was Test 3.

**Table E1. Maximum Internal and External Lower Chest Viscous Criteria and Proportionality Factors**

| Test | External VC | L Low. Chest IR-TRACC | L Low. Chest IR-TRACC | Proportionality Factor |
|---|---|---|---|---|
| # | *m/s* | *m/s* | *m/s* | - |
| 4 | 1.60 | 1.14 | 1.14 | 1.41 |
| 5 | 1.55 | 1.09 | 1.22 | 1.27 |
| 6 | 1.61 | 1.12 | 1.16 | 1.38 |

**Table E2. Maximum Internal and External Abdomen Viscous Criteria and Proportionality Factors**

| Test | External VC | L Abdomen IR-TRACC | R Abdomen IR-TRACC | Proportionality Factor |
|---|---|---|---|---|
| # | *m/s* | *m/s* | *m/s* | - |
| 1 | 1.74 | 1.73 | 1.57 | 1.01 |
| 2a | 1.74 | 1.53 | 1.41 | 1.14 |
| 3 | 1.80 | 1.48 | 1.43 | 1.22 |
| 16a | 1.74 | 1.56 | 1.41 | 1.12 |

The results of this limited study on abdomen VC and chest VC proportionality factors in the THOR-50M will be used in technical discussions within the APTA PR CS Working Group during revisions to APTA PR-CS-S-018. Preliminary findings do not appear to warrant changes to the chest VC proportionality factor, as the current proportionality factor (1.3) is within one standard deviation of the average lower chest VC measured in this study for the THOR-50M.

While the average abdomen VC proportionality factor estimated in this study appears to be larger than the current proportionality factor (1.0) currently used in the referenced standards, interference from the ASIS parts makes it difficult to interpret the results. All of the impacts to the abdomen IR-TRACCs (Tests 1, 2a, 3, 16a) exceeded the proposed deflection limit (84 mm); however, none of these tests exceeded the abdomen VC limit. This indicates that the current performance limit of abdomen VC (1.98 m/s) might be artificially high (see Appendix D – Viscous Criterion), or the proportionality factor (1.0) might be artificially low. There is evidence to support both of these claims that should be investigated further.

## Abbreviations and Acronyms

| ACRONYM | EXPLANATION |
|---|---|
| AIS | Abbreviated Injury Scale |
| APTA | American Public Transportation Association |
| ASIS | Anterior Superior Iliac Spine |
| ATD | Anthropomorphic Test Device |
| CFC | Channel Frequency Class |
| CG | Center of Gravity |
| CRUX | Compact Rotary Unit |
| CS | Construction and Structural |
| DAS | Data Acquisition Software |
| DGSP | Double Gimballed String Potentiometer |
| FE | Finite Element |
| FRA | Federal Railroad Administration |
| GESAC | General Engineering and Systems Analysis Co |
| H3-50M | Hybrid-III 50$^{th}$ Percentile Male |
| H3-RS | Hybrid-III Rail Safety |
| IARV | Injury Assessment Reference Value |
| IIHS | Insurance Institute for Highway Safety |
| IR-TRACC | Infra-red Telescoping Rod for Assessment of Chest Compression |
| L | Left |
| NCAP | New Car Assessment Program |
| NHTSA | National Highway Traffic Safety Administration |
| NI | National Instruments |
| PADI | Procedures for Assembly, Disassembly, and Inspection |
| PR | Passenger Rail |
| R | Right |
| RSSB | Rail Safety and Standards Board |
| SAE | Society of Automotive Engineers |
| SP | String Potentiometer |
| THOR-50M | Test Device for Human Occupant Restraint 50$^{th}$ Percentile Male |
| TRL | Transport Research Laboratory |

| ACRONYM | EXPLANATION |
|---|---|
| VC | Viscous Criterion |
| VRTC | Vehicle Research and Test Center |